LA-UR- 97-1087

Approved for public release; distribution is unlimited.

Title: SPECTRAL GAMMA-RAY LOG DATA ANALYSIS FOR NTS BOREHOLE ER-20-6 #1

Author(s): John G. Conaway, NIS-6

Submitted to:

HH

Los Alamos
NATIONAL LABORATORY

Form 836 (10/96)

DISCLAIMER

SPECTRAL GAMMA-RAY LOG DATA ANALYSIS FOR NTS BOREHOLE ER-20-6 #1

John Conaway
Los Alamos National Laboratory

SUMMARY

The Western Atlas spectral gamma-ray logs from borehole ER20-6 #1 seem to represent normal industry technology and practices. It is known from earlier experiments at the Atlas research facility in Houston that the computed artificial nuclide curves give a fairly reliable indication of zones where artificial gamma emitters are present but are not completely accurate in identifying *which* nuclides are present and which are not. In earlier data analysis efforts and the Houston experiments, we identified a number of deficiencies in the Atlas logging system and software that may contribute to this problem. Some of these deficiencies could be reduced by careful adjustments but, to a large extent, data quality seems to be limited by the low energy resolution inherent in the CsI detector used, and this cannot easily be changed.

One new problem identified in our data analysis for borehole ER20-6 #1 is that photopeaks from artificial nuclides apparently perturb the automatic spectral recalibration performed by Atlas in the post-processing stage. This leads to degraded calibration and probably degraded accuracy in nuclide identification in the zones of greatest interest in the UGTA work, those contaminated by artificial gamma emitters. This problem can probably be fixed or improved with relatively little effort.

The Western Atlas spectral gamma-ray computed nuclide curves from ER20-6 #1 indicate two major zones of radioactivity from artificial gamma emitters, a small but active zone around 1900 ft, and a longer zone of lesser activity from about 2028 to 2566 ft. The bluelines identify the zone at 1900 ft as being mostly ^{137}Cs with lesser amounts of ^{106}Ru, ^{125}Sb, and ^{134}Cs. We concur with the identification of ^{137}Cs but did not find any evidence of the other nuclides. Instead, we noted that the characteristic single ^{137}Cs photopeak had been incorrectly shifted on the energy axis by the Atlas automatic recalibration routine. While the other nuclides may be present in small quantities, it is likely that this energy shift also lead to some misidentification by the Atlas automatic full-spectral processing.

The curve plots identify the extended zone from 2028 to 2566 ft as being largely ^{106}Ru with lesser amounts of ^{137}Cs and ^{125}Sb. From our analysis of the spectra we conclude that artificial nuclides are definitely present in substantial quantities and the spectral shape is consistent with the Atlas results. However, the noise level in the processed spectrum is fairly high due to low spectral resolution and a number of small errors, so we cannot confirm this specific mix of nuclides with confidence. This radioactive material appears to be in the borehole fluid (i.e., formation water) or to have been spread by the borehole fluid. It seems unlikely that the zone at 1900 ft was the source for the contaminants below the water level in the zone from 2028 to 2566 ft because the artificial nuclide composition in these two zones are substantially different.

We recommend that the software problem that allows photopeaks from artificial nuclides to perturb the automatic spectral recalibration in the post-processing stage be fixed, and that the data then be reprocessed. This software fix should require a relatively minor effort and is especially important if more boreholes are to be logged in the UGTA work.

INTRODUCTION

In the characterization work underway at the Nevada Test Site Underground Test Area, the logging contractor, Western Atlas, has been asked to identify five artificial nuclides based on their gamma-ray signatures. Those nuclides are ^{60}Co (cobalt-60), ^{106}Ru (ruthenium-106), ^{125}Sb (antimony-125), ^{134}Cs (cesium-134), and ^{137}Cs (cesium-137). In the case of ^{106}Ru, which is not a gamma emitter, any detected gamma rays come from the daughter nuclide ^{106}Rh (rhodium-106) which has a half-life of 30 s. With such a short half-life, ^{106}Rh can be considered to be in equilibrium with ^{106}Ru under most conditions so the result is the same as if the gamma rays were emitted by the ^{106}Ru. Atlas does not attempt to provide a quantitative radioelement concentration estimate for the artificial nuclides. Log curves are expressed in counts per second attributed to each nuclide and additionally, for the artificial nuclides, as a per cent of the total count rate attributed to K, U, and Th. Although the Atlas tool is characterized for five artificial nuclides, other artificial gamma emitters may be present in a given borehole depending on the type of underground test and the elapsed time since the test was executed. For example, one artificial nuclide not included in the Atlas tool characterization was detected in the water samples from ER20-6 #1, ^{102m}Rh (rhodium-102 metastable).[1]

The Western Atlas spectral gamma-ray tool uses a 2 in by 12 in CsI(Na) (sodium-doped cesium iodide) scintillation detector. Cesium iodide has lower energy resolution than the better known sodium iodide scintillation material but is more rugged and is also more efficient, giving higher count rates especially at higher energies and potentially better counting statistics. Detected gamma rays are divided into 256 energy bins using a pulse-height analyzer in the tool, and the data are transmitted up the logging cable in digital form. Western Atlas personnel perform an energy calibration before and after each logging run using a calibration gamma-ray source. Atlas also performs a running adjustment of the spectral energy scale during the office post-processing based on the positions of known peaks in the naturally occurring spectral components; this is important and will be discussed in a later section.

SGR logging is potentially very sensitive, giving an estimated detection threshold better than 0.1 pCi/g for ^{137}Cs under good conditions. However, the conditions at the NTS are not ideal. At the NTS, the decision was made to use a scintillator-based logging system for operational reasons, in part because logging with high resolution detectors would be much more expensive. Much depends on the contractor's ability to extract subtle information from noisy, low-resolution gamma-ray spectra.

The Western Atlas spectral gamma-ray curve plots from a given borehole present detailed information on the apparent distribution of natural and artificial nuclides with depth in the borehole. If we were to perform a similar, foot-by foot analysis of the data we would have to develop complicated data processing routines requiring months of development and validation. Such an effort is beyond the scope of our funding and is redundant if the contractor's data processing is being performed correctly. A more efficient use of our limited resources is to

provide a quality analysis of the contractor's processed data and to work with the contractor to validate and/or refine their existing automatic processing. We do this using a procedure that was developed and tested successfully in earlier work at the NTS[2], as described in the next sections.

DATA VALIDATION FOR BOREHOLE ER-20-6 #1

Borehole ER20-6 #1 is located in Area 20 (Pahute Mesa) at the NTS near the site of the Bullion underground nuclear test. Bullion was conducted in June, 1990, at a depth of 2211 ft. Water samples and sidewall cores from ER20-6 #1 were analyzed by others[e.g. 1] for artificial gamma emitters (Tables 1 and 2).

Table 1. Radionuclides detected in water pumped from ER20-6b #1[1].

Nuclide	Activity (pCi/l)
^{106}Ru	406
^{125}Sb	183
^{137}Cs	39.8
^{102m}Rh	0.7
^{60}Co	0.4

Table 2. Radionuclides detected in core samples from ER20-6 #1[1].

Sample ID Number	Depth (ft)	^{137}Cs Activity (pCi/g)	^{125}Sb Activity (pCi/g)
2061-96-310	1890	1.1	
2061-96-320	1896	0.5	
2061-96-330	1907	380	21
2061-96-340	1915	0.6	
2061-96-350	2190	0.6	
2061-96-360	2205	1.6	
2061-96-370	2480	0.5	

To provide an independent assessment of data quality, we have divided the spectral gamma-ray log from borehole ER20-6 #1 into depth zones based on the distribution of artificial nuclides indicated on the curve plots. For reference, the curve data are plotted here as Figures 1 to 5, in 500 ft sections. These plots have a logarithmic count rate axis to show detail at the low count rate end without clipping at the high count rate end.

The curve plots show a major anomaly from about 2028 ft to 2566 ft (Figures 4 and 5) consisting largely of ^{106}Ru with some ^{125}Sb, according to Atlas. A smaller, hotter zone is indicated from about 1896 to 1911 ft (Figure 3), and a very small anomaly, still flagged as statistically significant, is located from 1527 to 1530 ft (Figure 3). Most of the remaining borehole is shown as being free of artificial nuclides ("clean") with the exception of a few small anomalies not flagged by Atlas as statistically significant. Our analysis of the data concentrated on spectra accumulated over each of these three anomalous zones flagged as statistically significant, along with spectra accumulated over remaining regions of the borehole indicated as clean.

Our overall impression from the blueline is that one entry point for contamination is in the high count rate zone around 1900 feet. The extended artificial nuclide anomaly from 2028 to 2566 ft is probably contamination distributed in the borehole fluid or spread by the borehole fluid (note that the fluid level at the time of logging was noted on the blueline header as 2029 ft). Again, the source of this contamination may have been the zone at 1900 ft, although the contamination in the zone from 2028 to 2566 ft appears to be a mix including ^{125}Sb and/or ^{106}Ru (the Atlas processing strongly indicates ^{106}Ru and the water analysis data are in agreement as shown in Table 1) while the anomaly at 1900 ft appears to be mostly or entirely ^{137}Cs (confirmed by the core data seen in Table 2). Thus, there may be an entry point below the water level, perhaps in the relatively high count rate region around 2200 ft. These zones of interest are considered in detail below.

Zone from 1896 - 1911 ft

Figure 6a shows the field spectrum accumulated from 1896 to 1911 ft in borehole ER20-6 #1 plotted on semi-log axes; the same information is plotted again in Figure 7a on a linear scale (the software used to perform these analyses is described in Appendix A). Figure 6b shows the same accumulated field spectrum (solid line) plotted along with the dotted line representing the thorium spectral template (again, plotted on a linear scale in Figure 7b). The vertical lines represent the expected positions of three photopeaks representative of the thorium family spectrum. The spectral template count rates have been scaled interactively to give a good fit over the prominent 2.614 MeV peak of ^{208}Tl (a daughter of ^{232}Th). Since no other photopeaks are expected in that energy range, we can confidently perform this fit and subtract the scaled spectral template from the accumulated field spectrum. It should be noted that ^{106}Rh, the daughter of ^{106}Ru, has gamma rays of energies up to 3.4 MeV but with negligible yields.

The remaining field spectrum after the scaled thorium template has been subtracted is plotted as the solid line in Figures 6c and 7c; the dotted line in both plots is the uranium spectral template. The vertical lines represent the expected positions of three uranium family photopeaks. Again, the template has been interactively fitted to the higher-energy uranium peaks; since the contribution of thorium has been subtracted, uranium-family peaks in the range of 2.2 to 2.4 MeV should now be the only important high-energy peaks.

Notice that there is some noise visible in the remaining field spectrum after subtracting the scaled thorium template, including two small negative peaks visible in Figure 7c around 2.3 - 2.7 MeV (because Figure 6c has a semi-log axis, negative count rates cannot be displayed and count rates below 0.01 count per s have been truncated). This noise results largely from an imperfect fit between the spectral template and the field spectrum, including small errors in computing and applying the instrument energy calibration (gain and offset) and differences in the shape of the

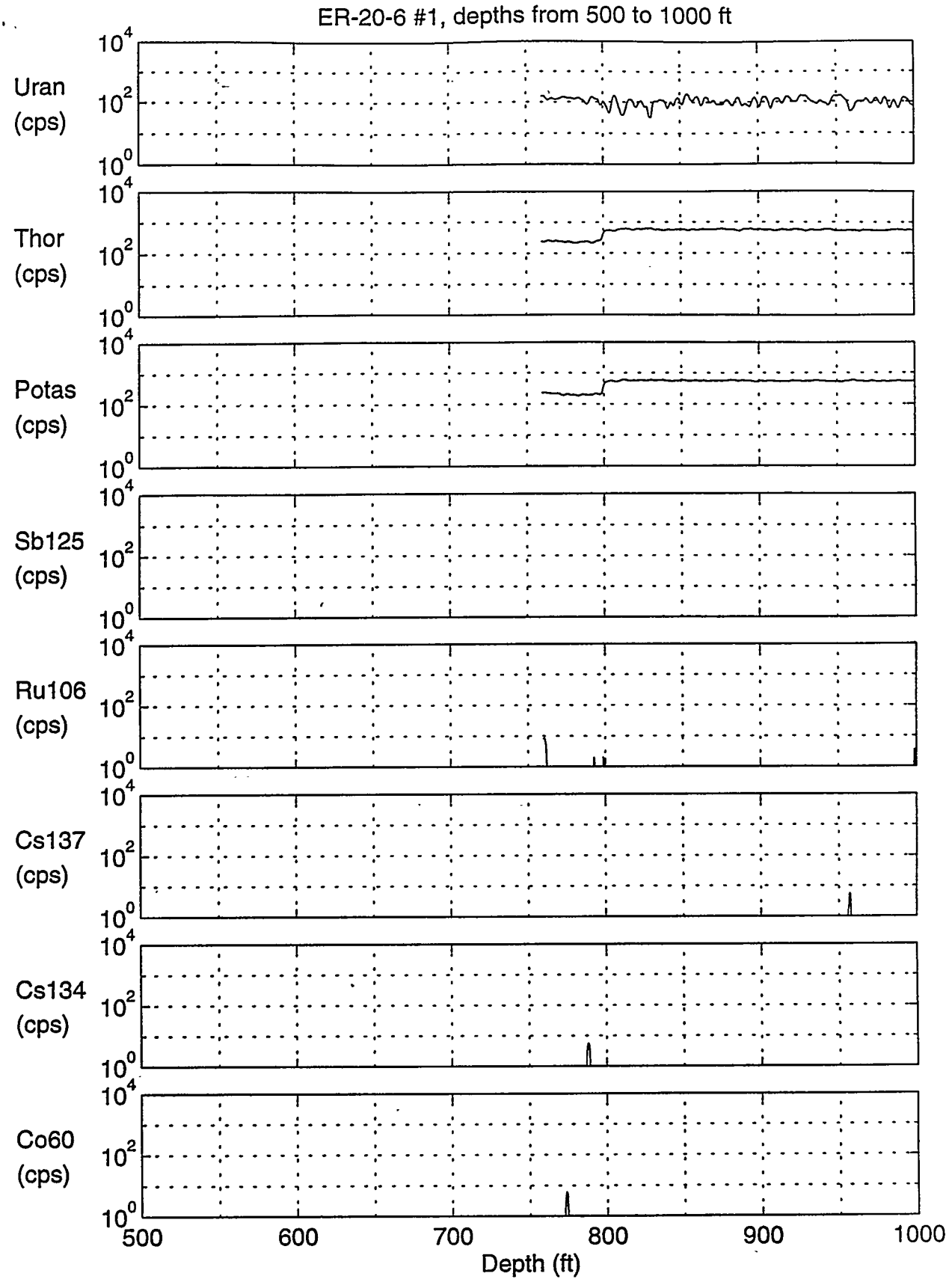

Figure 1. Western Atlas curve data for 500 - 1000 ft.

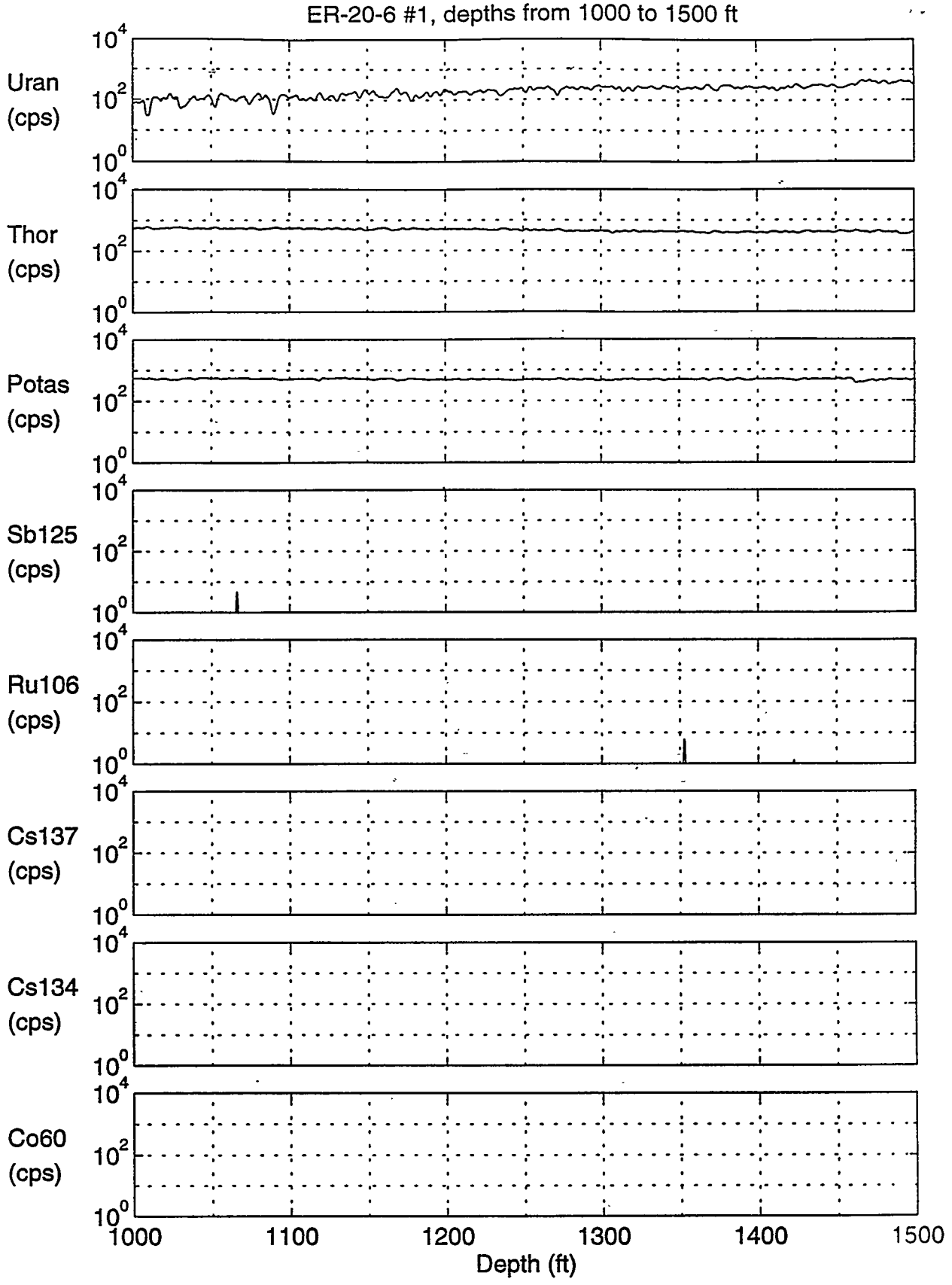

Figure 2. Western Atlas curve data for 1000 - 1500 ft.

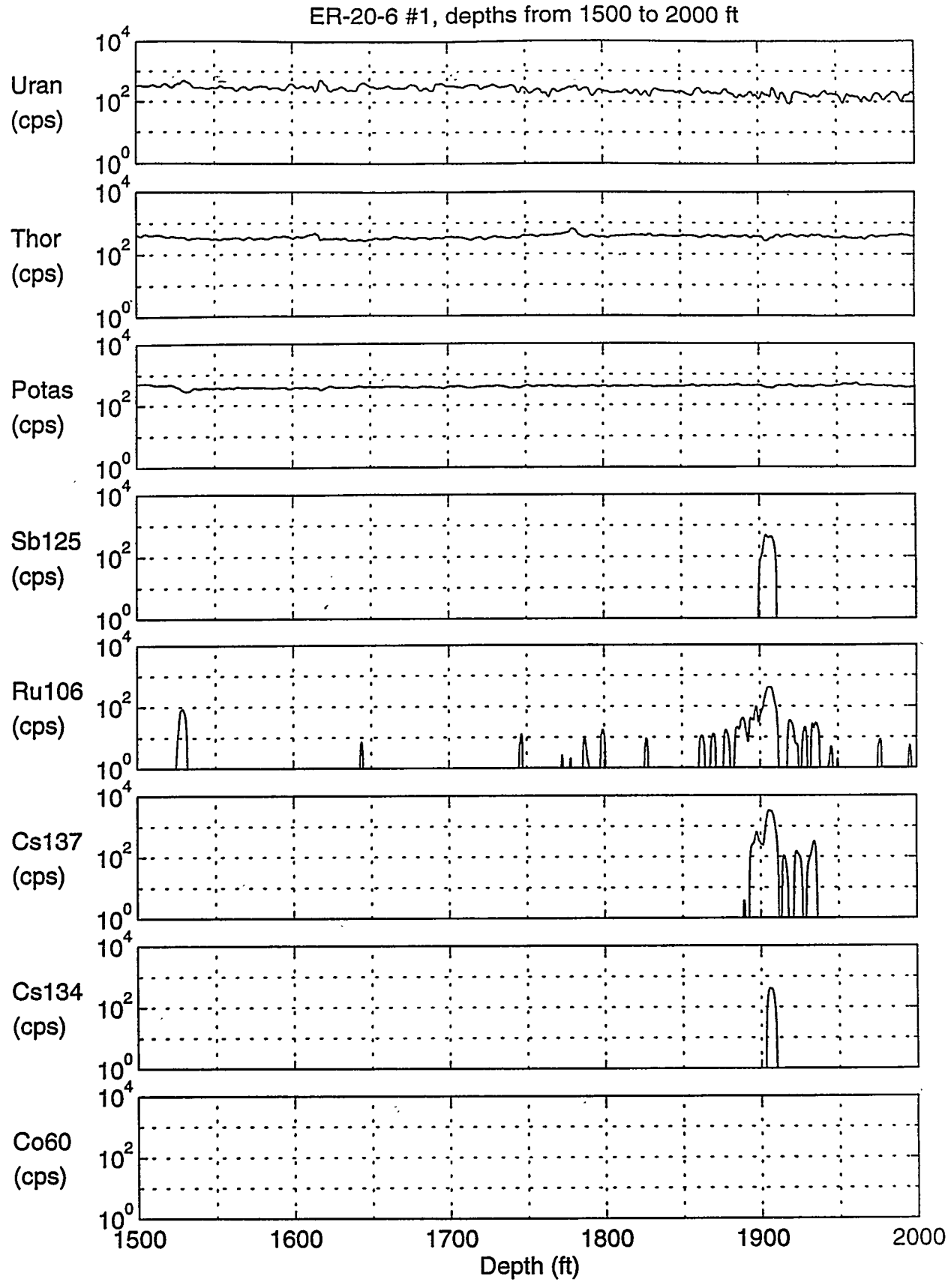

Figure 3. Western Atlas curve data for 1500 - 2000 ft.

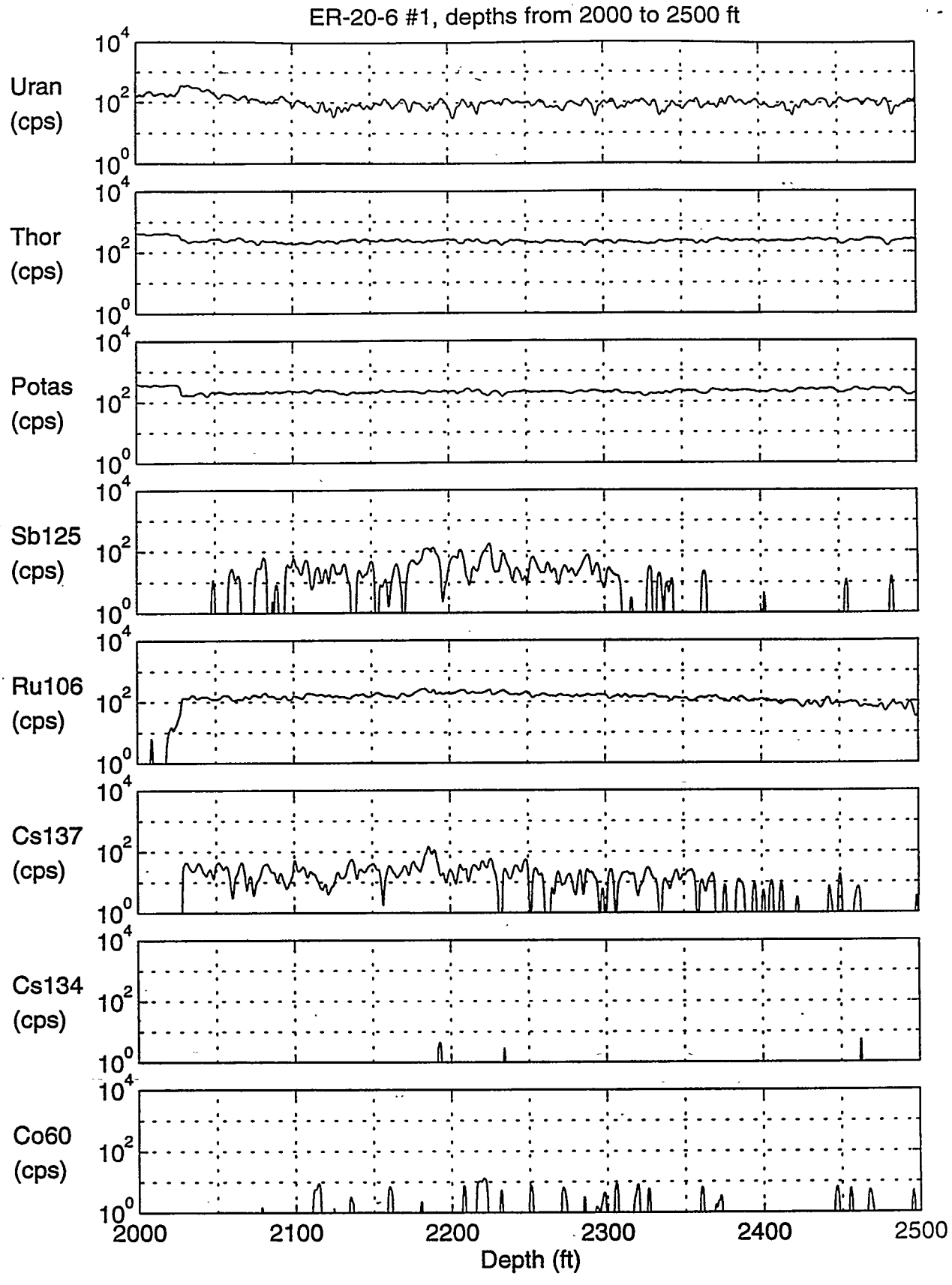

Figure 4. Western Atlas curve data for 2000 - 2500 ft.

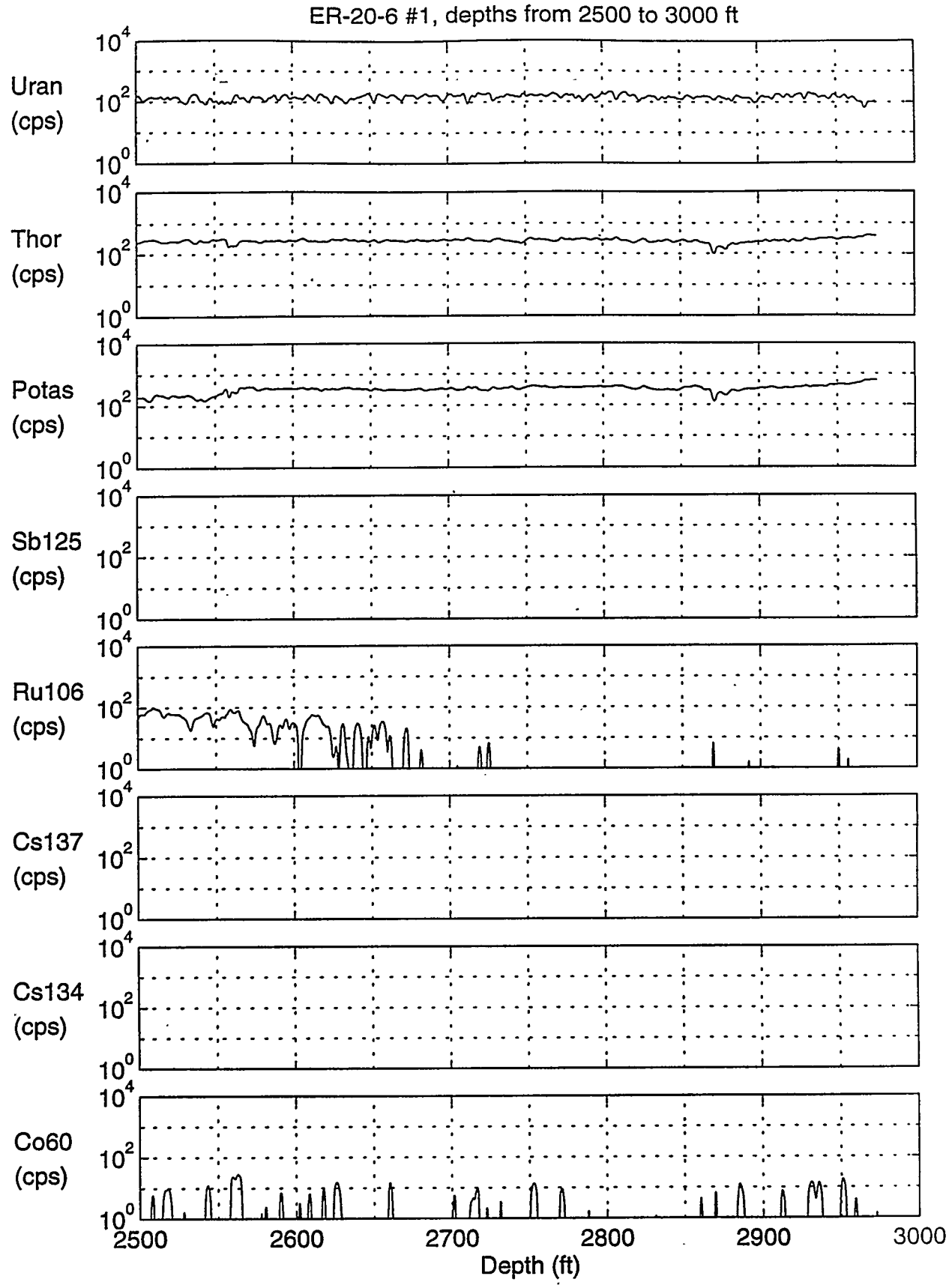

Figure 5. Western Atlas curve data for 2500 - 3000 ft.

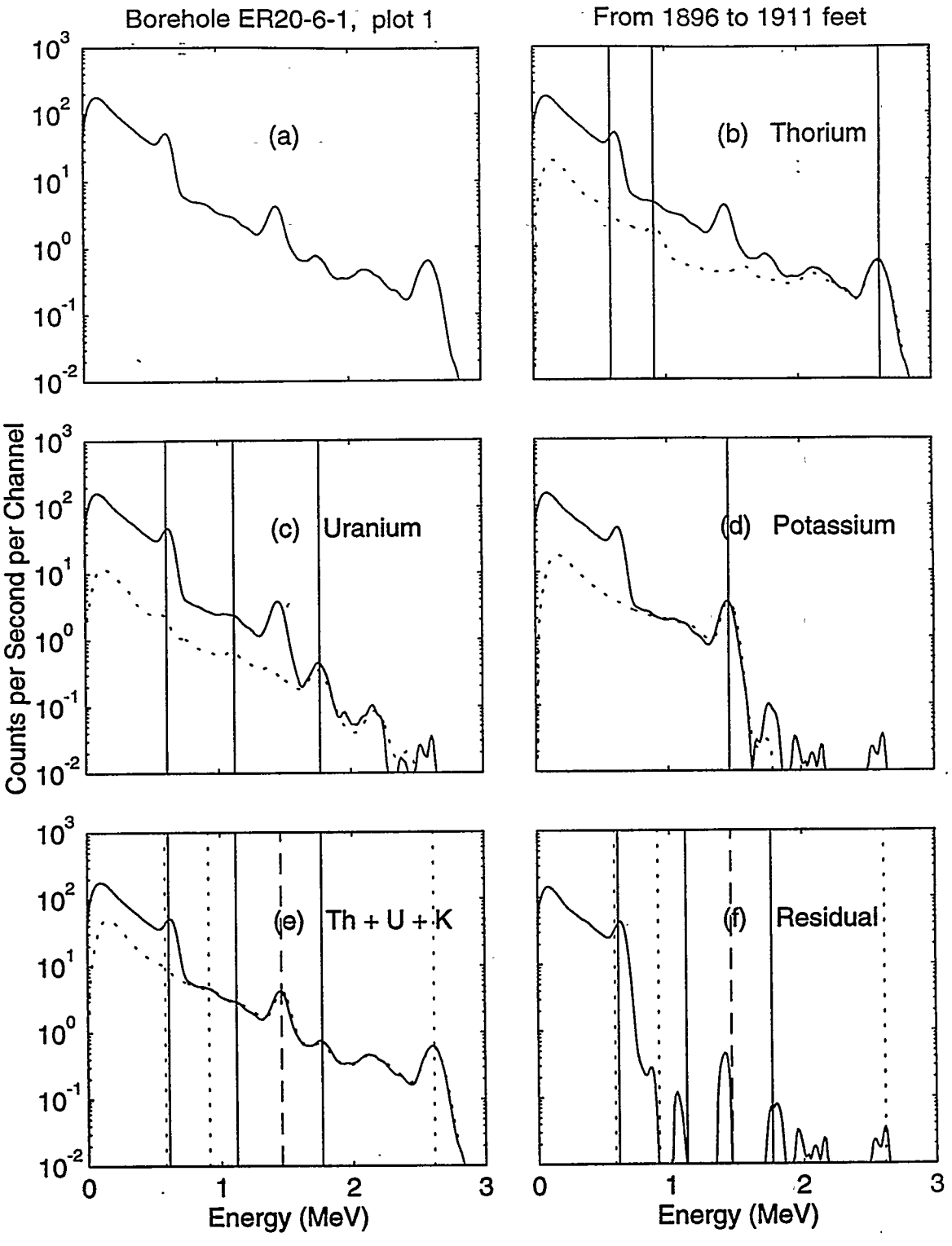

Figure 6. Field spectrum accumulated from 1896 to 1911 ft in borehole ER20-6 #1 plotted on semi-log axes. The various stages of data processing described in the text are shown.

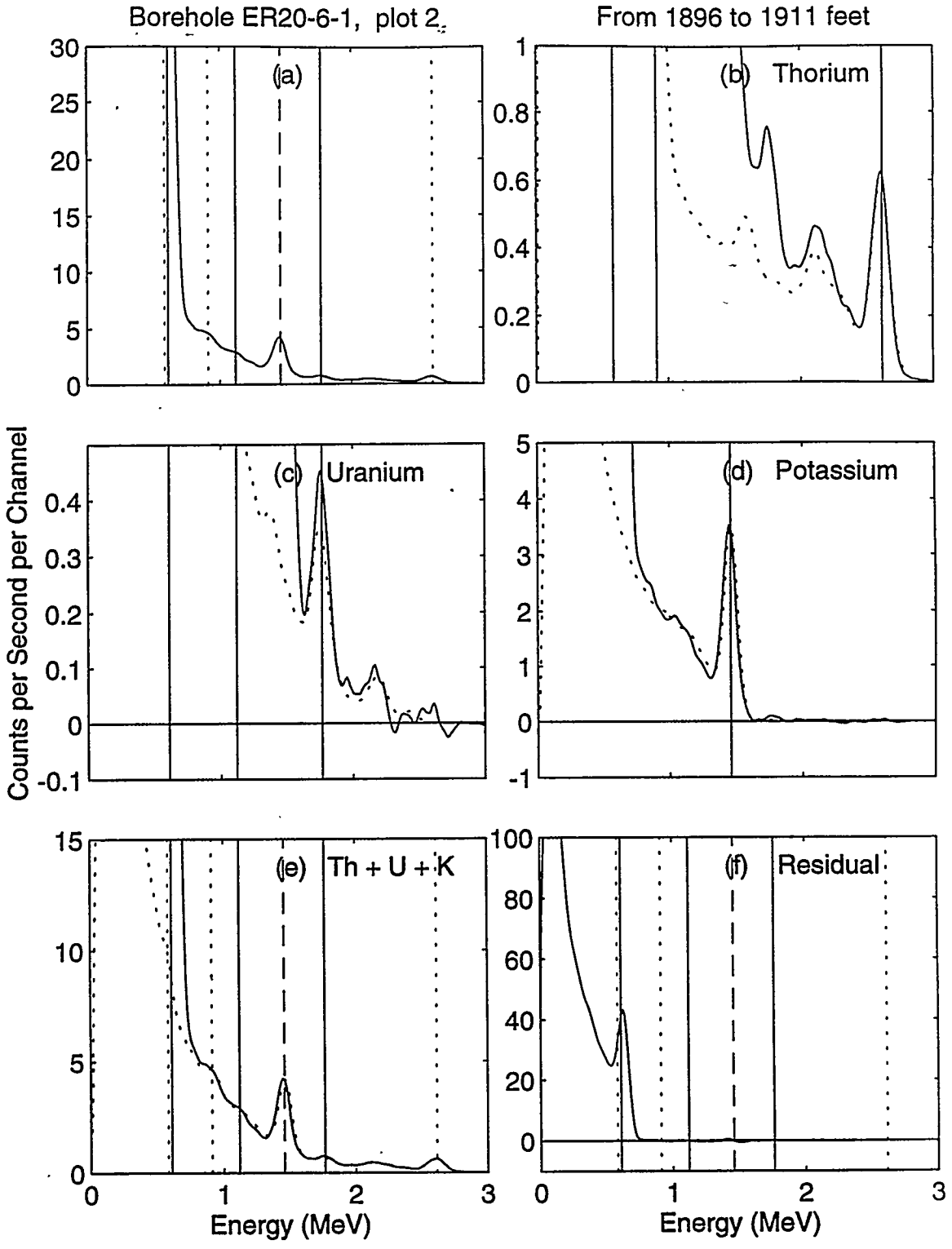

Figure 7. Field spectrum accumulated from 1896 to 1911 ft in borehole ER20-6 #1 plotted on linear axes. The various stages of data processing described in the text are shown.

spectra because the calibration borehole environment was not the same as the field borehole environment. While negative count rates may seem troubling, they are simply an indication of imperfection in the data processing and they provide an indication of the noise level.

Subtracting the scaled uranium spectral template from the remaining field spectrum leads to the solid line in Figures 6d and 7d. The vertical line represents the expected position of the single ^{40}K photopeak. The dotted line in both figures is the potassium spectral template, scaled interactively to fit over the single potassium photopeak around 1.46 MeV. Several artificial gamma-emitters of interest at the NTS also produce photons in this energy range so some trial and error may be required at this stage.

Once again, subtracting the scaled (potassium) spectral template from the remaining field spectrum produces the *residual* spectrum shown in Figures 6f and 7f. Since we have subtracted the scaled spectral templates corresponding to the known natural gamma-emitters, the residual spectrum includes any artificial components plus noise. In this case, the residual spectrum seems to correspond rather clearly to a monoenergetic gamma emitter. The vertical lines represent expected positions for some representative photopeaks of the natural spectrum, solid for uranium family, dotted for thorium family, and dashed for ^{40}K.

At this point we can perform another check to see how well the natural spectral components explain the shape of the field spectrum. In Figures 6e and 7e, the original accumulated field spectrum is plotted as the solid line; the dotted line represents the sum of the scaled spectral templates corresponding to the natural gamma emitters. These plotted curves correspond fairly closely at energies above about 0.7 MeV but there is a substantial amount of gamma activity evident below that energy that cannot be explained by any combination of the natural gamma emitters.

In a case like this where artificial nuclides are present, the next stage in the analysis is to try to determine which nuclides they are. First, the residual spectrum is plotted alone (Figures 8a and 9a) and in combination with spectral templates corresponding to each of the five artificial gamma emitters (Figures 8b - 8f and 9b - 9f). Based on inspection of these plots, we conclude that the bulk of the signal is from ^{137}Cs with its characteristic single photopeak at 0.662 MeV, although that peak seems to be shifted slightly toward lower energies. The shape of the residual spectrum simply does not agree with the multi-peak shapes of the other artificial nuclide templates. This conclusion is in agreement with the Western Atlas curve plots that show largely ^{137}Cs around 1900 ft in the borehole (Figure 3).

The curve plots also show lesser signals from ^{125}Sb, ^{106}Ru, and ^{134}Cs that are still flagged as statistically significant. Although one or more of those materials may be present, the quality of the field data and the Atlas spectral analysis software are not adequate to detect low concentrations of those materials in the presence of high concentrations of ^{137}Cs with any confidence. A small amount of ^{125}Sb was found in the core sample at 1907 ft (Table 2) but no ^{106}Ru or ^{134}Cs was reported.

After some investigation, we have concluded that the apparent energy shift in the 0.662 MeV ^{137}Cs peak is an artifact of the Western Atlas automatic energy adjustment algorithm. This is discussed in the section titled *"automatic energy calibration,"* later in this report.

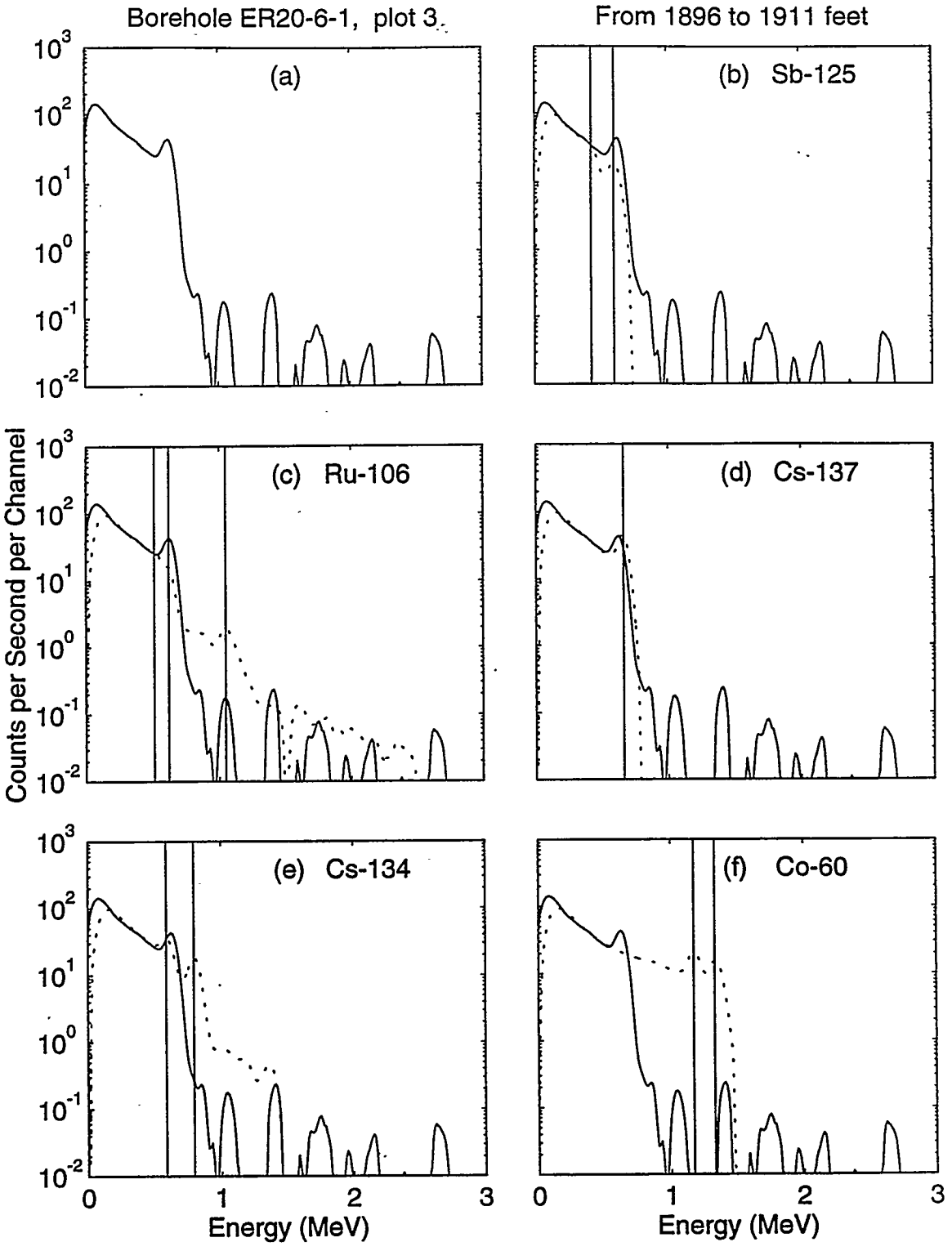

Figure 8. Processed spectrum accumulated from 1896 to 1911 ft in borehole ER20-6 #1 plotted on semi-log axes showing the effect of artificial nuclides as described in the text.

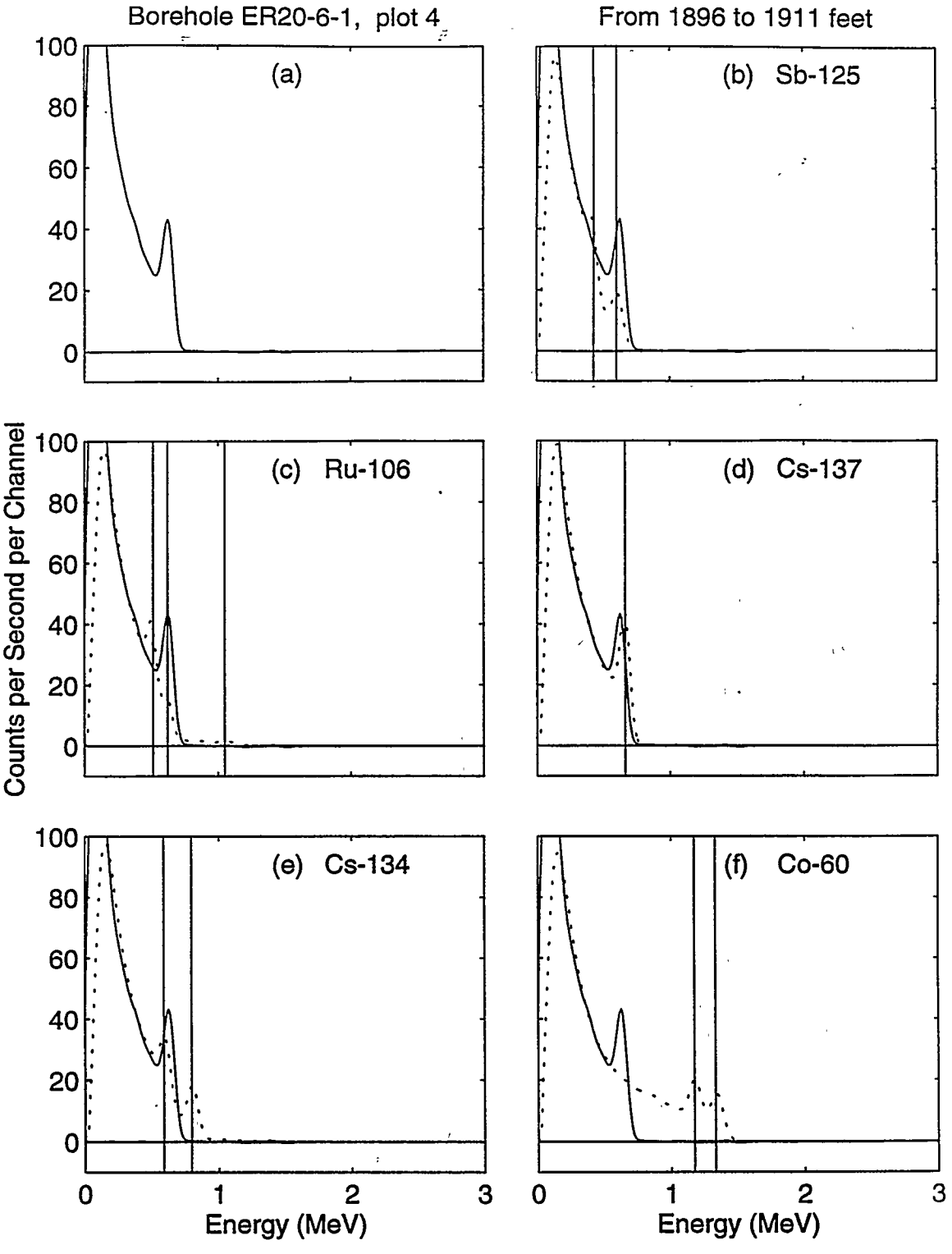

Figure 9. Processed spectrum accumulated from 1896 to 1911 ft in borehole ER20-6 #1 plotted on linear axes showing the effect of artificial nuclides as described in the text.

Zone from 2028 - 2566 ft

The data processing procedure is the same as followed in the example above (1896 - 1911 ft) and will not be described in as much detail here. Figure 10a shows the field spectrum accumulated from 2028 to 2566 ft and the same information is plotted in Figure 11a on a linear scale. Figure 10b shows the same accumulated field spectrum (solid line) plotted along with the dotted line representing the thorium spectral template (again, plotted on a linear scale in Figure 11b).

The remaining field spectrum after the scaled thorium template is subtracted is plotted as the solid line in Figures 10c and 11c; the dotted line in both plots is the uranium spectral template. Subtracting the scaled uranium spectral template from the remaining field spectrum leads to the solid line in Figures 10d and 11d; the dotted line in both figures is the potassium spectral template.

Once again, subtracting the scaled (potassium) spectral template from the remaining field spectrum produces the residual spectrum shown in Figures 10f and 11f. In Figures 10e and 11e, the original accumulated field spectrum is plotted as the solid line while the dotted line represents the sum of the scaled spectral templates corresponding to the natural gamma emitters. These plotted curves correspond fairly closely at higher energies but the effect of artificial gamma emitters is once again evident at the low-energy end of the field spectrum.

Continuing with the analysis, the residual spectrum is plotted alone (Figures 12a and 13a) and in combination with spectral templates corresponding to each of the five artificial gamma emitters (Figures 12b - 12f and 13b - 13f). There are some suggestive similarities in overall shape and peak position, but the overall noise level is too high to discern individual nuclides with confidence. Based on the shape of the residual spectrum, one or more of ^{125}Sb, ^{137}Cs, and particularly ^{106}Ru, is present. ^{134}Cs and ^{60}Co are probably not present or are present in very small concentrations. Water pumped from this zone contained ^{106}Ru, ^{125}Sb, and ^{137}Cs, along with trace quantities of ^{102m}Rh and ^{60}Co (Table 1).

Zone from 1527 - 1530 ft

Figure 14a shows the field spectrum accumulated from 1527 to 1530 ft and the same information is plotted in Figure 15a on a linear scale. Figure 14b shows the same accumulated field spectrum (solid line) plotted along with the dotted line representing the thorium spectral template (again, plotted on a linear scale in Figure 15b).

The remaining field spectrum after the scaled thorium template is subtracted is plotted as the solid line in Figures 14c and 15c; the dotted line in both plots is the uranium spectral template. Subtracting the scaled uranium spectral template from the remaining field spectrum leads to the solid line in Figures 14d and 15d; the dotted line in both figures is the potassium spectral template.

Once again, subtracting the scaled (potassium) spectral template from the remaining field spectrum produces the residual spectrum shown in Figures 14f and 15f. In Figures 14e and 15e, the original accumulated field spectrum is plotted as the solid line while the dotted line represents the sum of the scaled spectral templates corresponding to the natural gamma emitters. These curves correspond fairly closely at higher energies but the effect of artificial gamma emitters is once again evident at the low-energy end of the field spectrum.

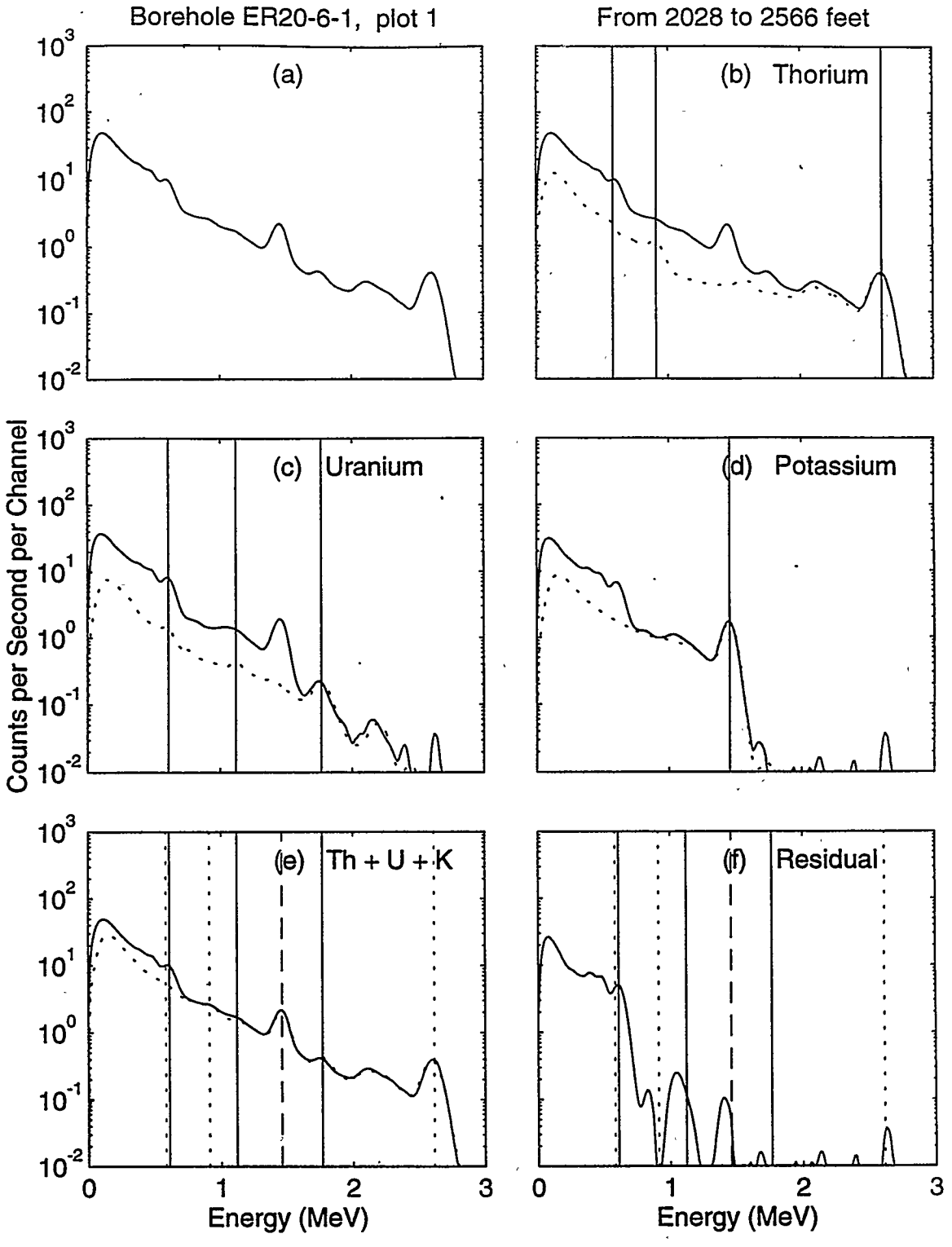

Figure 10. Field spectrum accumulated from 2028 to 2566 ft in borehole ER20-6 #1 plotted on semi-log axes. The various stages of data processing described in the text are shown.

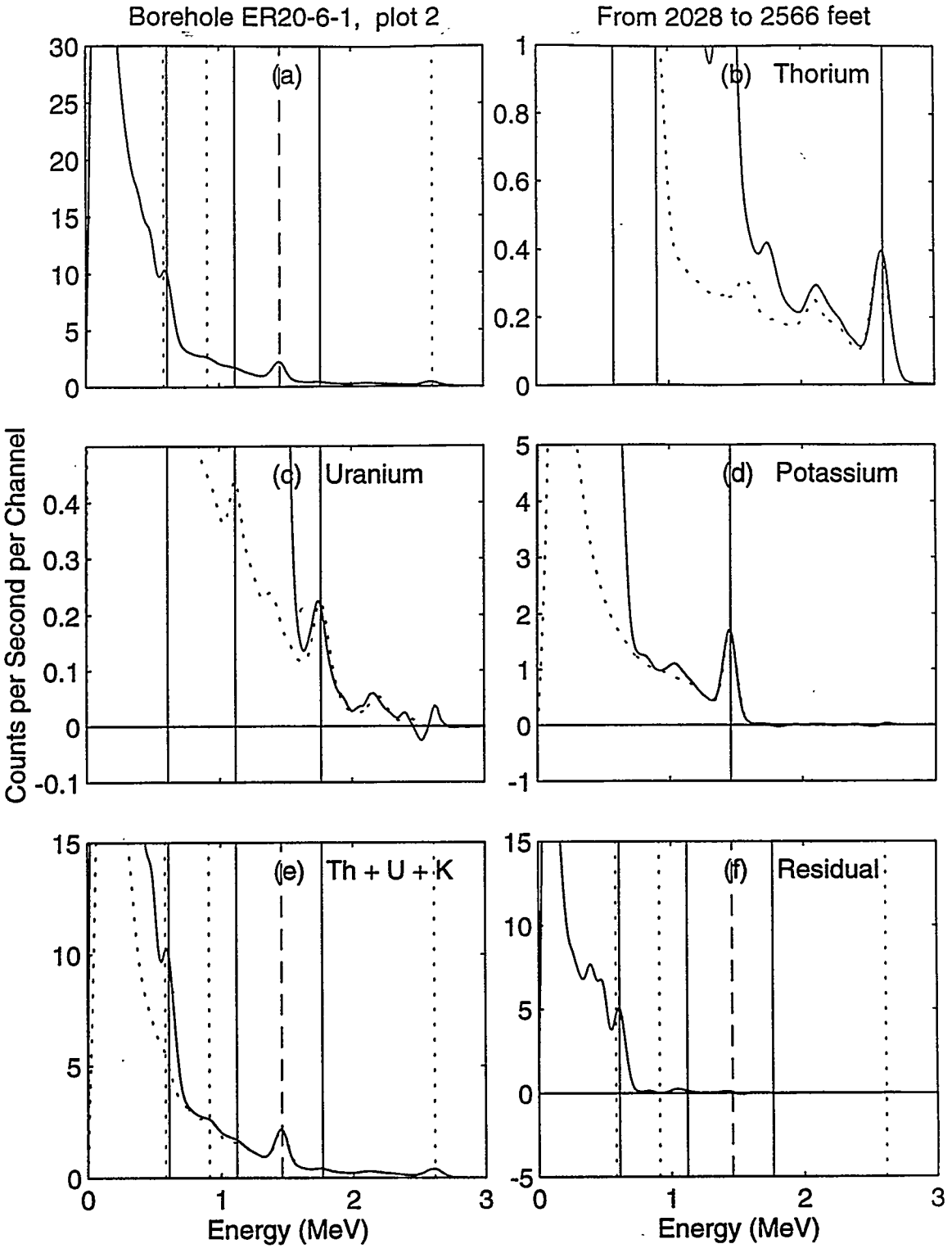

Figure 11. Field spectrum accumulated from 2028 to 2566 ft in borehole ER20-6 #1 plotted on linear axes. The various stages of data processing described in the text are shown.

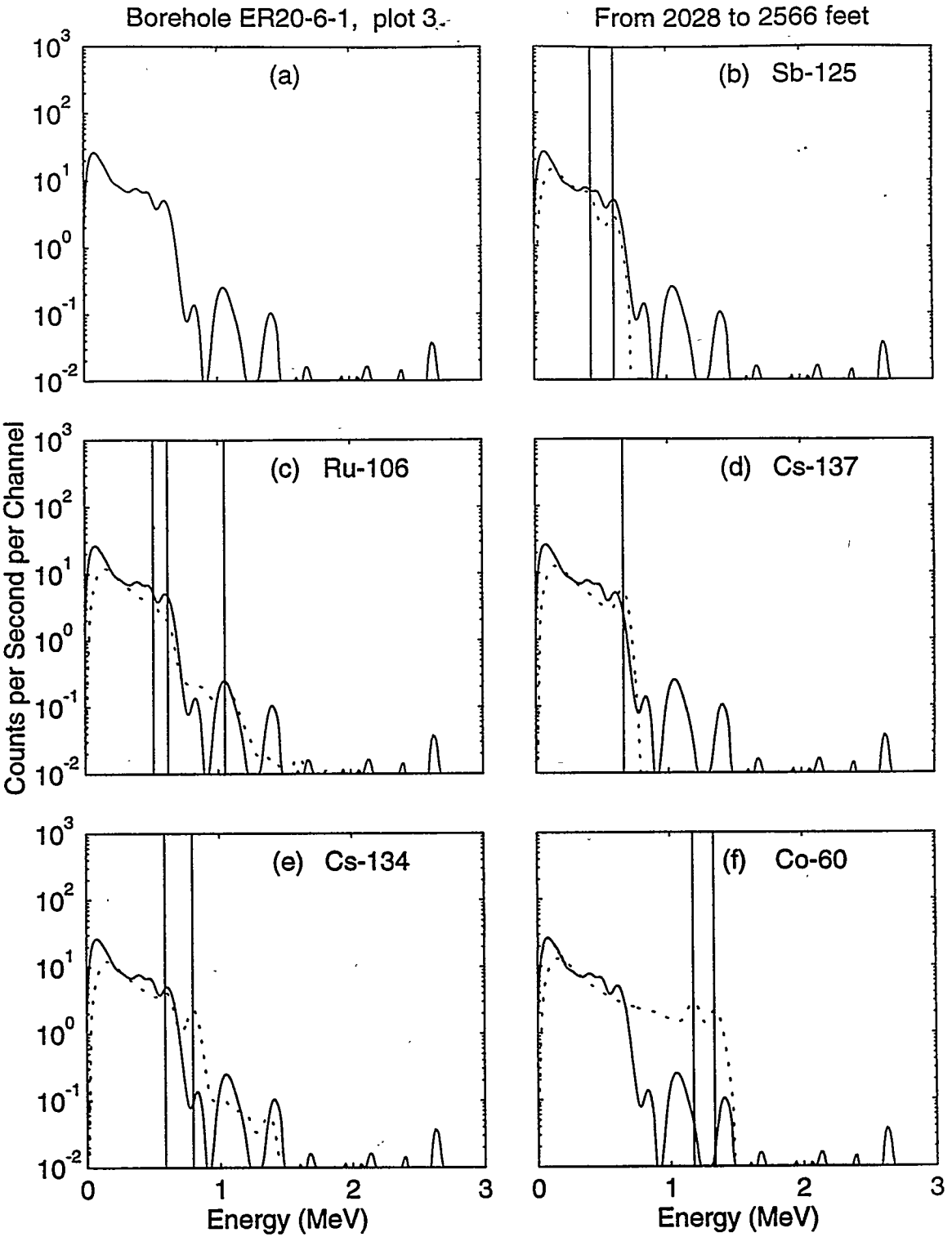

Figure 12. Processed spectrum accumulated from 2028 to 2566 ft in borehole ER20-6 #1 plotted on semi-log axes showing the effect of artificial nuclides as described in the text.

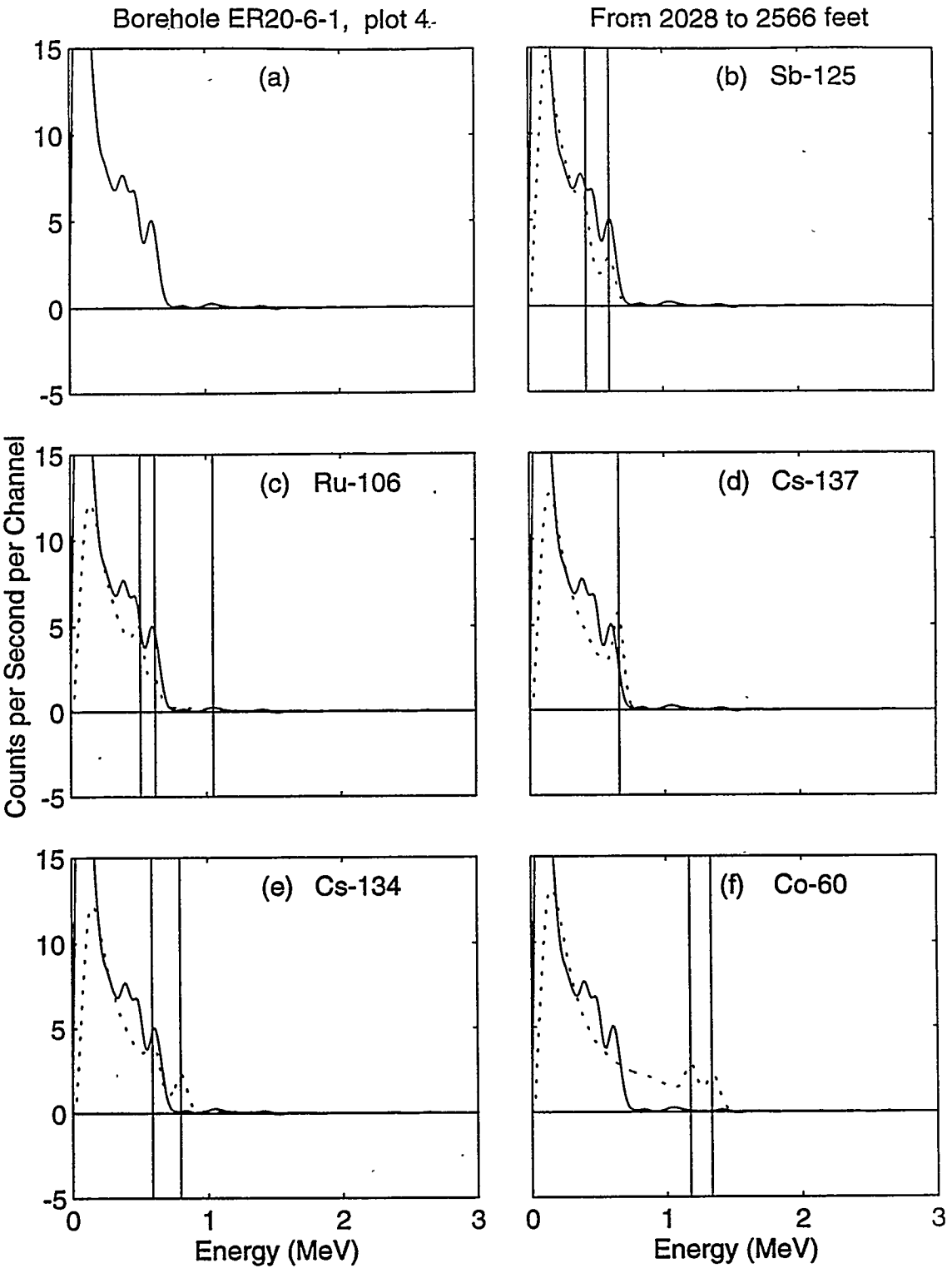

Figure 13. Processed spectrum accumulated from 2028 to 2566 ft in borehole ER20-6 #1 plotted on linear axes showing the effect of artificial nuclides as described in the text.

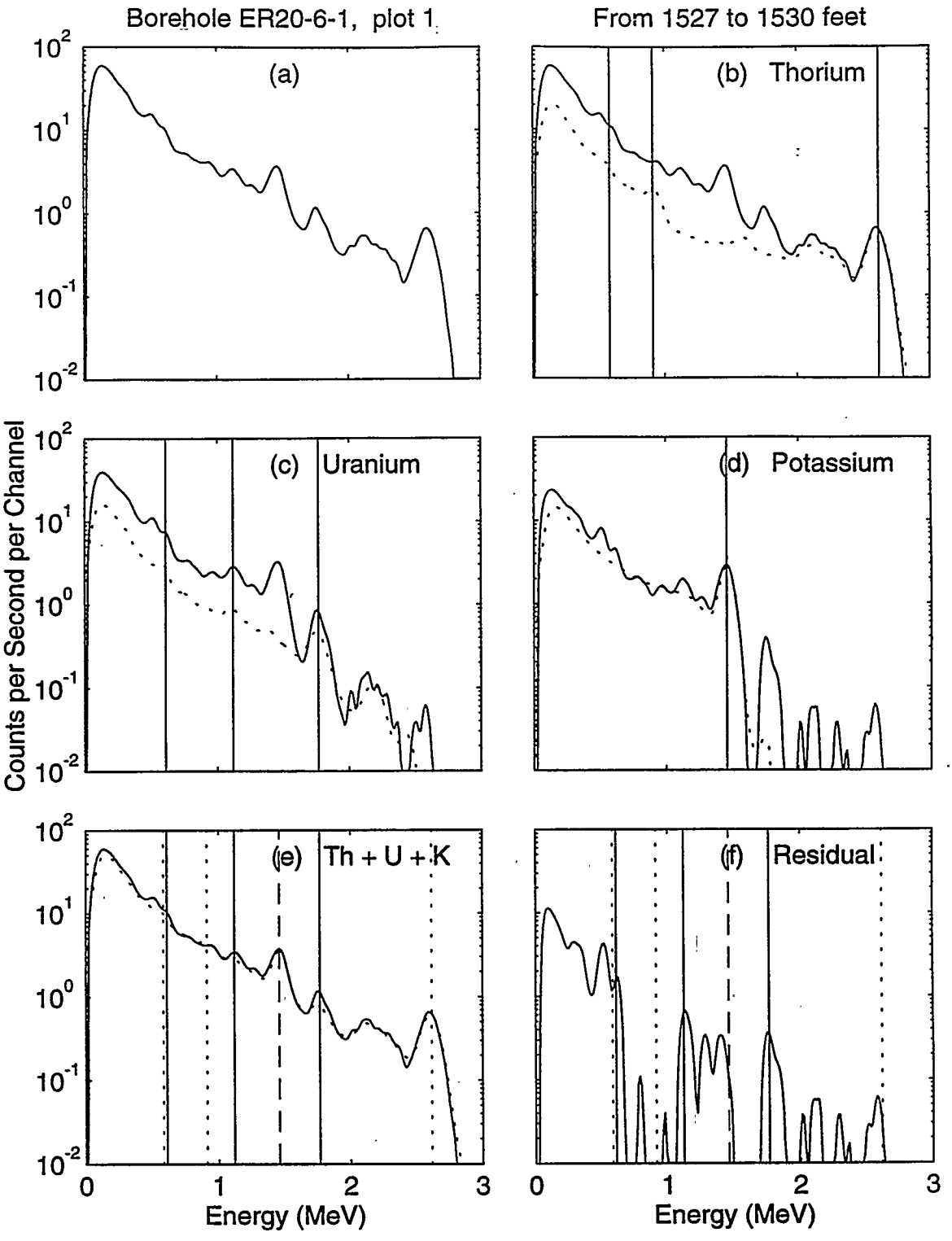

Figure 14. Field spectrum accumulated from 1527 to 1530 ft in borehole ER20-6 #1 plotted on semi-log axes. The various stages of data processing described in the text are shown.

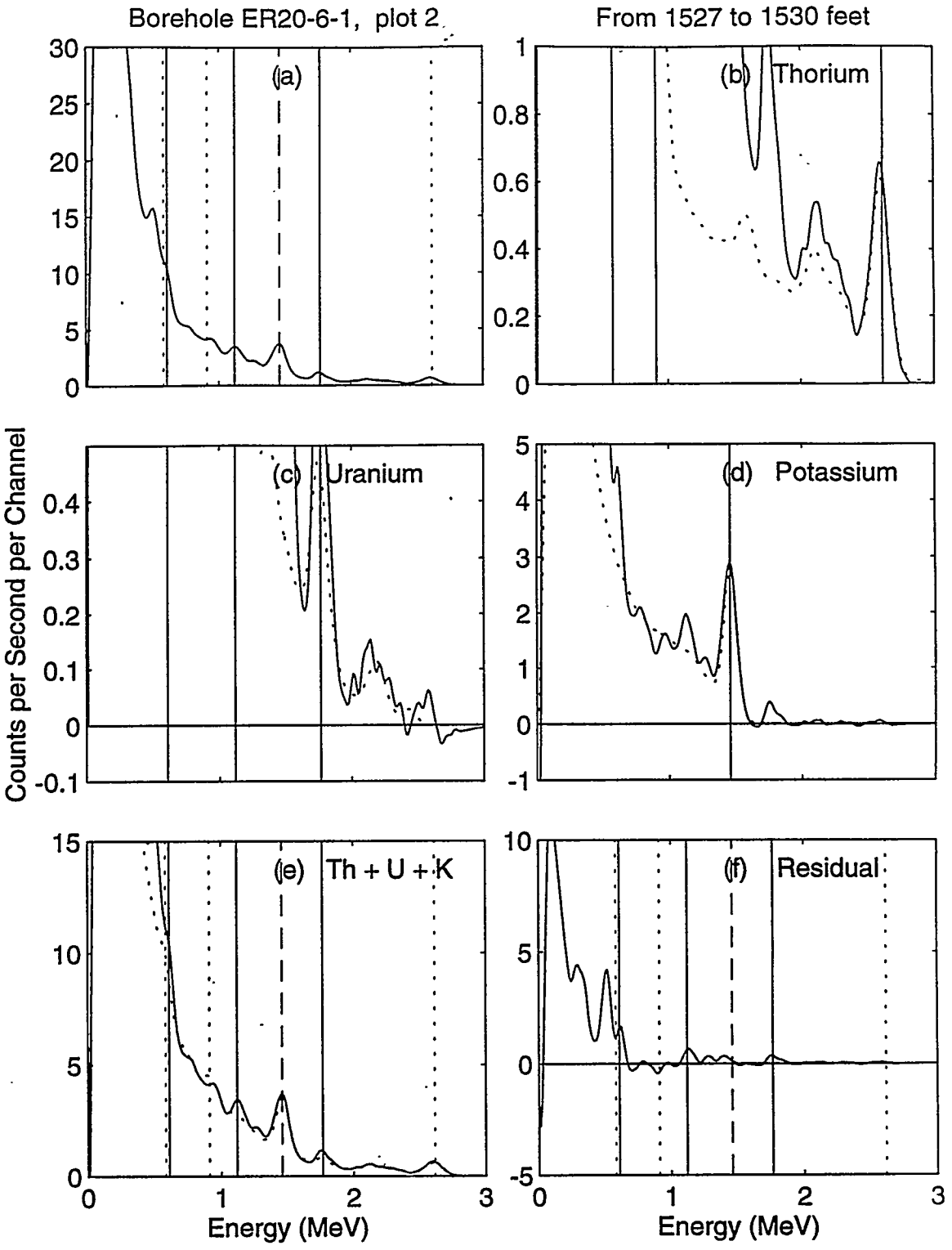

Figure 15. Field spectrum accumulated from 1527 to 1530 ft in borehole ER20-6 #1 plotted on linear axes. The various stages of data processing described in the text are shown.

The residual spectrum is plotted in combination with spectral templates corresponding to each of the five artificial gamma emitters (Figures 16b - 16f and 17b - 17f). This zone is indicated on the curve plots (Figure 3) as a small anomaly and the noise level in the spectrum is high. It appears likely that artificial nuclides are present but any attempt to identify specific nuclides would be problematic and probably misleading.

Clean zones

Figure 18a shows the field spectrum accumulated over all clean regions of borehole ER20-6 #1 plotted on semi-log axes; the same information is plotted on a linear scale in Figure 19a. Figures 18b and 19b show the same accumulated field spectrum (solid line) plotted along with the thorium spectral template (dotted). The remaining field spectrum after the scaled thorium template has been subtracted is plotted as the solid line in Figures 18c and 19c; the dotted line in both plots is the uranium spectral template. Again, there is some noise visible in the remaining field spectrum, including the negative peak visible in Figure 19c around 2.6 - 2.7 MeV; this noise results from an imperfect fit between the spectral template and the field spectrum.

Subtracting the scaled uranium spectral template from the remaining field spectrum leads to the solid line in Figures 18d and 19d; the dotted line is the potassium spectral template. Once again, subtracting the scaled (potassium) spectral template from the remaining field spectrum produces the residual spectrum shown in Figures 18f and 19f. Since we have subtracted the scaled spectral templates corresponding to the known natural gamma-emitters, the residual spectrum includes any artificial components plus noise.

At this point we can check to see how well the natural spectral components explain the shape of the field spectrum. In Figures 18e and 19e, the original accumulated field spectrum is plotted as the solid line; the dotted line represents the sum of the scaled spectral templates corresponding to the natural gamma emitters, potassium and the uranium and thorium families. These plotted curves correspond fairly closely and we can conclude that the shape of the field spectrum is well explained by natural radiation – there is no sign of significant levels of artificial nuclides. We also examined data from some of the individual clean zones with similar results.

Looking again at the residual spectrum (Figure 19f) we immediately note several features, a peak at low energy, a negative excursion, and some small peaks and troughs. All of these features can be adequately explained, once again, as resulting from an imperfect fit between the spectral templates and the field spectrum due to differing instrumental and measurement conditions. The negative excursion occurs in the energy range where most of the artificial nuclides lie, so any significant quantity of these materials would tend to eliminate that negative excursion. These errors are due largely to differences between field conditions and the calibration conditions under which the spectral templates were derived; these differences contribute to the problem of identifying artificial nuclides using the Atlas SGR borehole data.

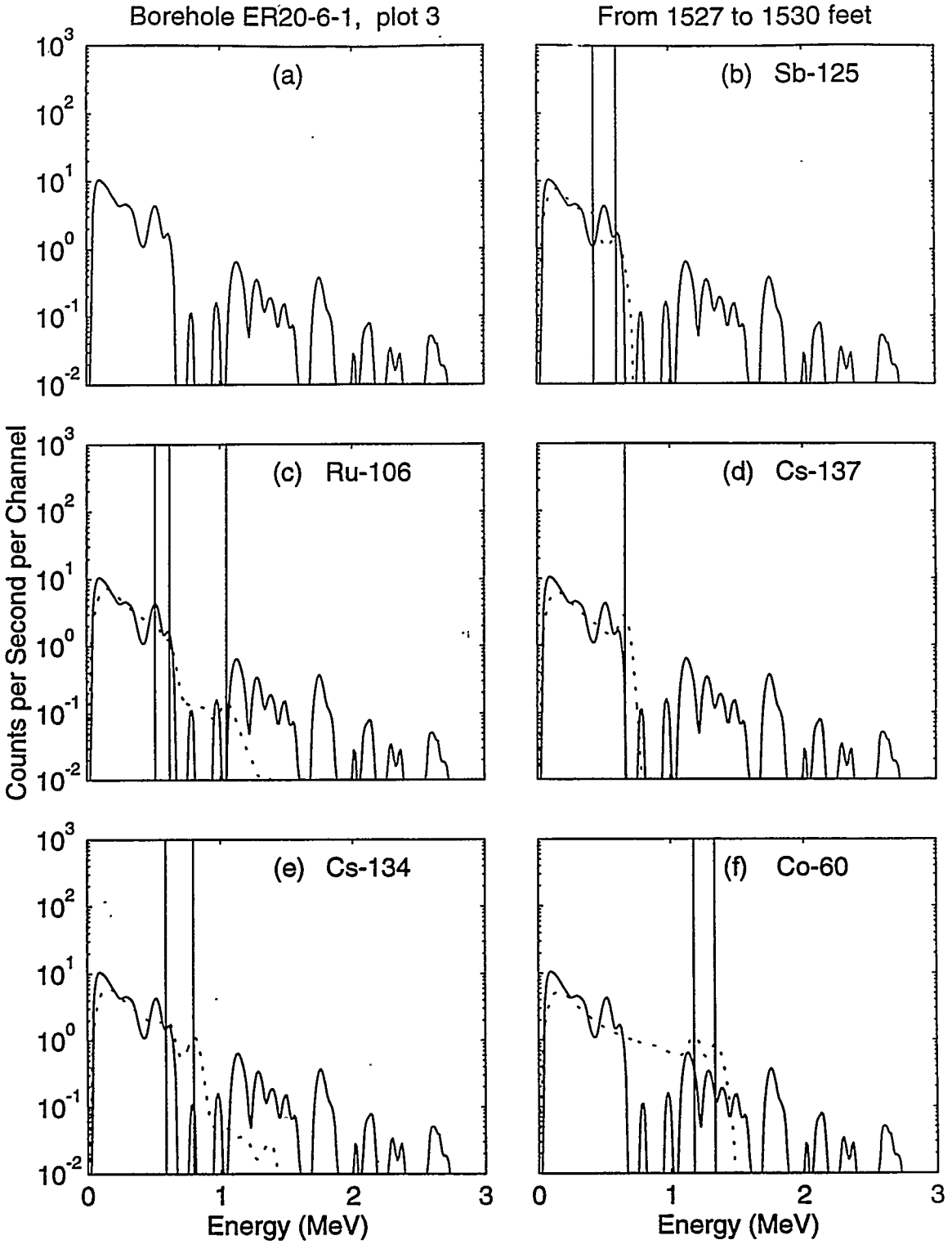

Figure 16. Processed spectrum accumulated from 1527 - 1530 ft in borehole ER20-6 #1 plotted on semi-log axes showing the effect of artificial nuclides as described in the text.

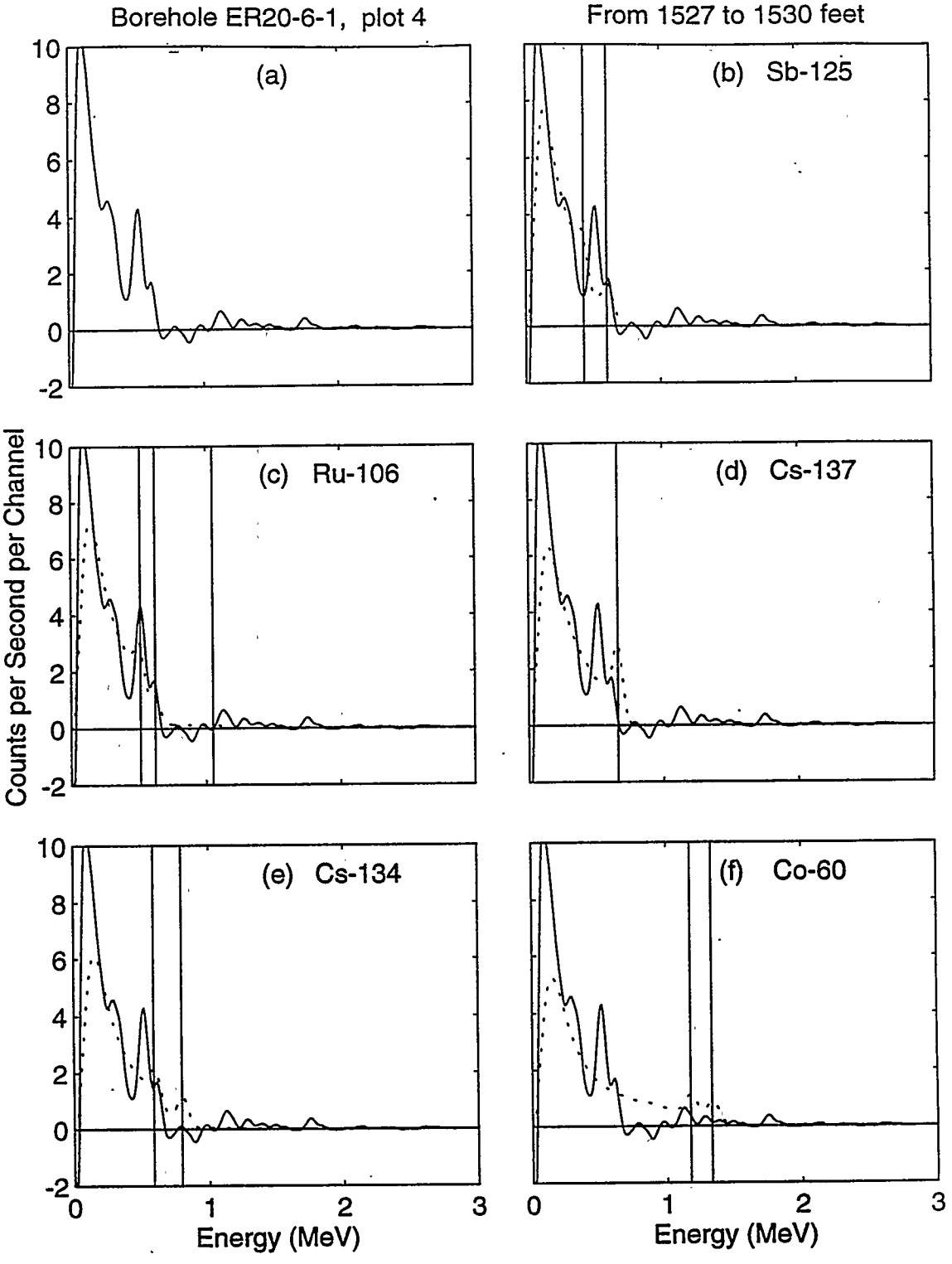

Figure 17. Processed spectrum accumulated from 1527 - 1530 ft in borehole ER20-6 #1 plotted on linear axes showing the effect of artificial nuclides as described in the text.

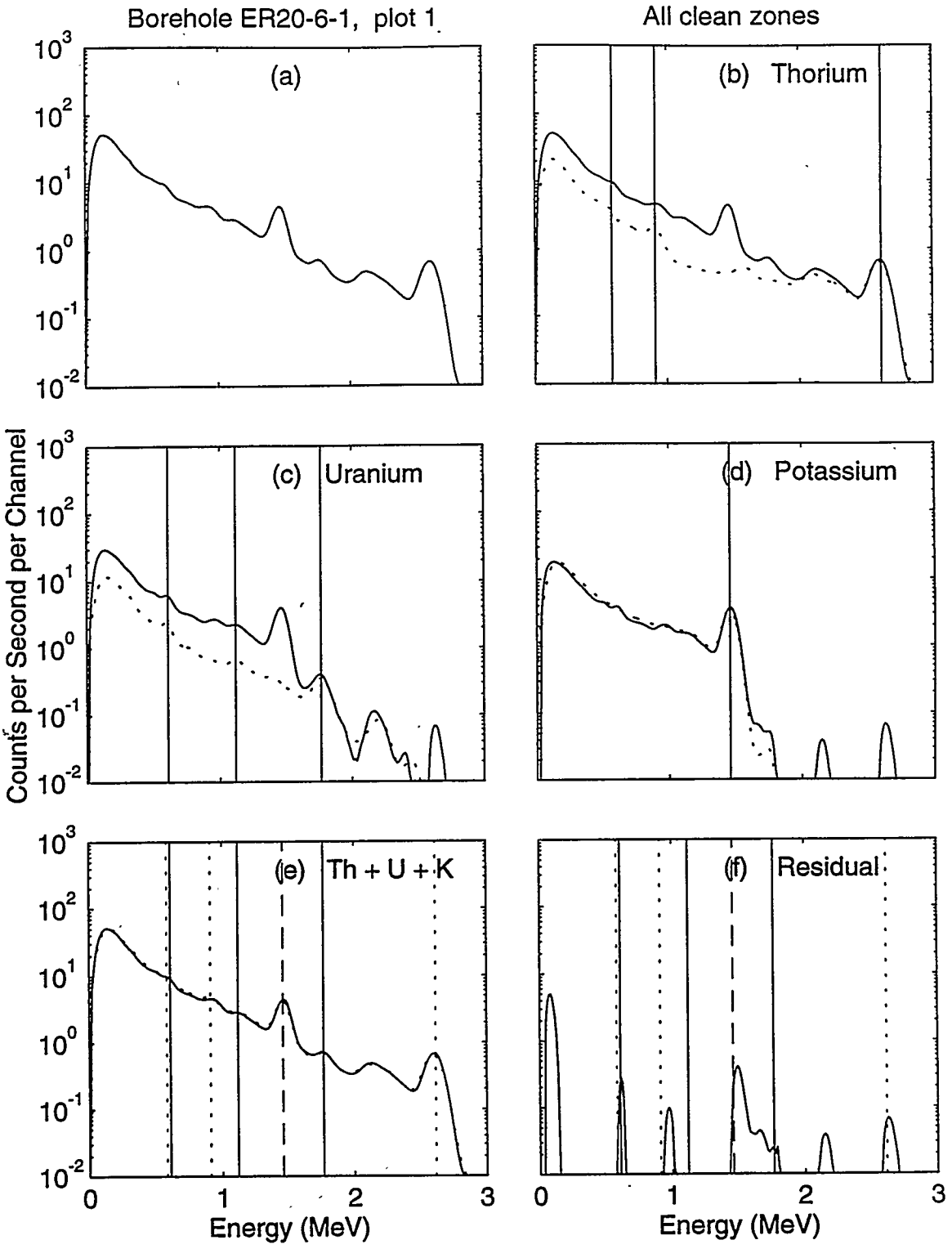

Figure 18. Field spectrum accumulated from all clean zones in borehole ER20-6 #1 plotted on semi-log axes. The various stages of data processing described in the text are shown.

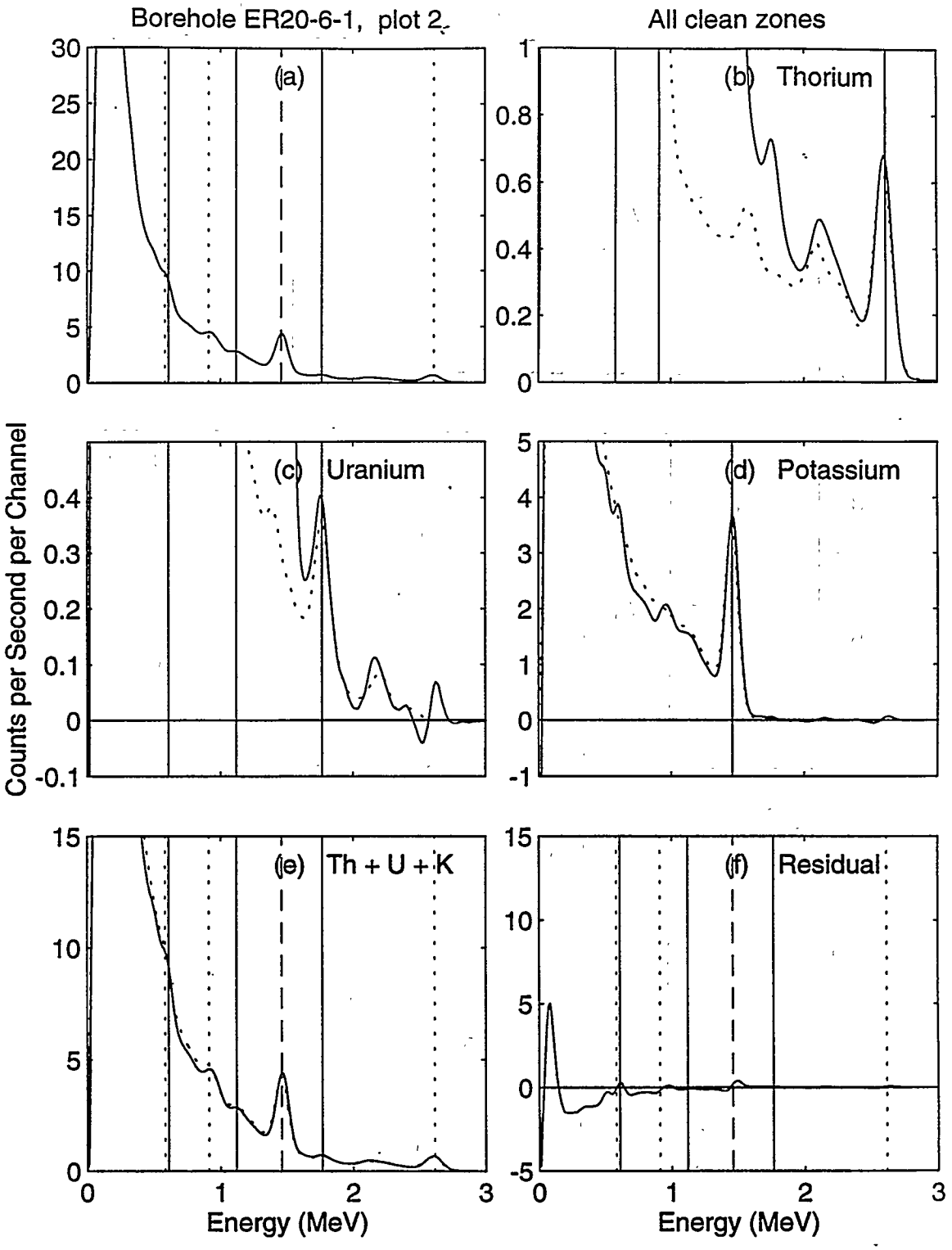

Figure 19. Field spectrum accumulated from all clean zones in borehole ER20-6 #1 plotted on linear axes. The various stages of data processing described in the text are shown.

PROBLEMS WITH THE AUTOMATIC ENERGY CALIBRATION

In the analysis of the anomaly around 1900 feet, we noted a significant energy shift in the position of the 0.662 MeV ^{137}Cs peak in the residual spectrum (e.g. Figure 7f). The Western Atlas post-processing software uses automatic peak tracking to monitor and adjust the spectral energy calibration. Overall, the Western Atlas automatic energy adjustment algorithm seems to work fairly well but it was designed for clean boreholes; when artificial nuclides are present there seems to be a problem, which is discussed in this section. Other potential problems with the Atlas logging system and data processing were discussed in an earlier report and are listed in Appendix B.

One of the peaks tracked by the Atlas post-processing energy calibration routine is the 0.609 MeV peak of ^{214}Bi, a daughter of ^{238}U. Because of the low energy resolution of the CsI detector, this 0.609 MeV peak and the 0.662 MeV ^{137}Cs peak merge into one somewhat broader peak that the automatic peak tracking routine is likely to use as its 0.609 MeV reference, thereby incorrectly shifting the calculated spectral offset and gain parameters. Thus, in the recalibrated (residual) spectrum (Figure 7f) the 0.662 MeV photopeak of ^{137}Cs has been shifted closer to the 0.609 MeV position of ^{214}Bi expected by the automatic peak tracking software. This is not the only possible interference of artificial nuclides peaks with the natural reference peaks used in the automatic calibration routine. Table 3 lists the five reference calibration peaks from natural gamma emitters along with photopeaks from the five artificial nuclides considered here that might cause an apparent shift in the reference peaks.

Table 3. The 5 natural gamma-ray peaks used as reference peaks in the Atlas spectral processing, listed with the artificial nuclide gamma-ray peaks that may interfere with them.

REFERENCE PEAKS		POSSIBLE INTERFERENCE FROM	
ENERGY (MeV)	NUCLIDE	ENERGY (MeV)	NUCLIDE
0.352	^{214}Pb	0.428	^{125}Sb
0.609	^{214}Bi	0.662	^{137}Cs
		0.601	^{125}Sb
		0.636	^{125}Sb
		0.622	^{106}Ru
		0.587	^{134}Cs
1.461	^{40}K	1.333	^{60}Co
		1.365	^{134}Cs
1.765	^{214}Bi	none	-
2.614	^{208}Tl	none	-

In the Atlas post-processing, a calibration spectrum is summed over the first 50 ft of log and the quality control tests and calibration adjustments, if any, for a point centered in that 50 ft section

are based on that summed spectrum. Spectra from successive sample depths are added into the calibration spectrum and spectra are subtracted at the same rate from the other end of the 50 ft interval so the calibration spectrum always represents a spectrum accumulated over a 50 ft interval centered on the current depth.[3]

Figures 20 - 24 show plots of the Atlas quality control parameters for borehole ER20-6 #1 along with the artificial nuclide curves. The quality control parameters are described briefly in Table 4. Especially noteworthy here is the pronounced change in spectral gain (QMSL) and offset (QASL) in the vicinity of the strong artificial anomaly around 1900 ft. This seems to be a fairly convincing illustration of the interference of an artificial nuclide peak (the 0.662 MeV ^{137}Cs peak) with a spectral calibration reference peak (the 0.609 MeV ^{214}Bi peak), resulting in erroneous calibration values for a roughly 50-ft region centered on that zone. This erroneous spectral calibration reduces the chance that the Atlas automatic full-spectral processing software will correctly determine which artificial nuclides that are actually present and which are not.

Table 4. The Atlas spectral calibration and quality control parameters discussed in the text.

PARAMETER	DESCRIPTION
QMSL	Multiplicative energy calibration factor (gain, M).
QASL	Additive energy calibration factor (offset, A).
QPKS	Number of specified spectral reference peaks recognized by the calibration routine (out of a possible 5 peaks). Normally QPKS must be at least 4 for an automatic recalibration to be performed.
QCAL	Slope of the line obtained by performing linear regression on a plot of measured reference peak channels (y-axis) against expected reference peak channels (x-axis).
QSA	Chi-squared test describing goodness-of-fit of the reference peak channels versus energy plot. Normally, QSA must be less than 1 for an automatic recalibration to be performed

CONCLUSIONS AND RECOMMENDATIONS

The Western Atlas spectral gamma-ray logs from borehole ER20-6 #1 seem to represent normal industry technology and practice. The computed artificial nuclide curves give a fairly reliable indication of clean zones and zones where artificial gamma emitters are present but are not completely accurate in identifying *which* nuclides are present and which are not in the contaminated zones. In earlier data analysis efforts and experiments at the Atlas research facility in Houston, we identified a number of deficiencies in the Atlas logging system and software that contribute to this problem (Appendix B). Some of these deficiencies could be reduced by careful adjustments but, to a large extent, data quality is limited by the low energy resolution inherent in the CsI detector used, and this cannot easily be changed.

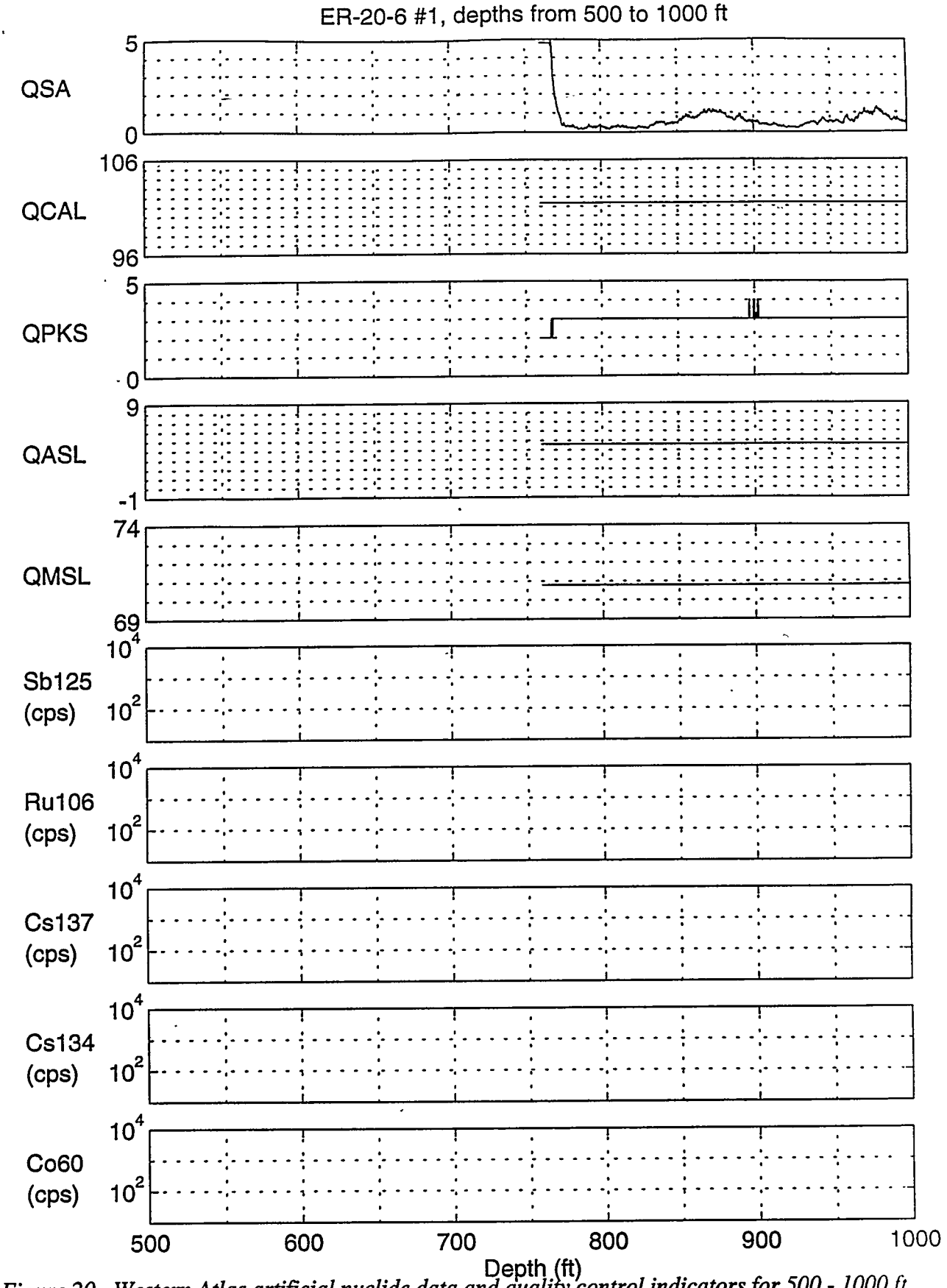

Figure 20. Western Atlas artificial nuclide data and quality control indicators for 500 - 1000 ft.

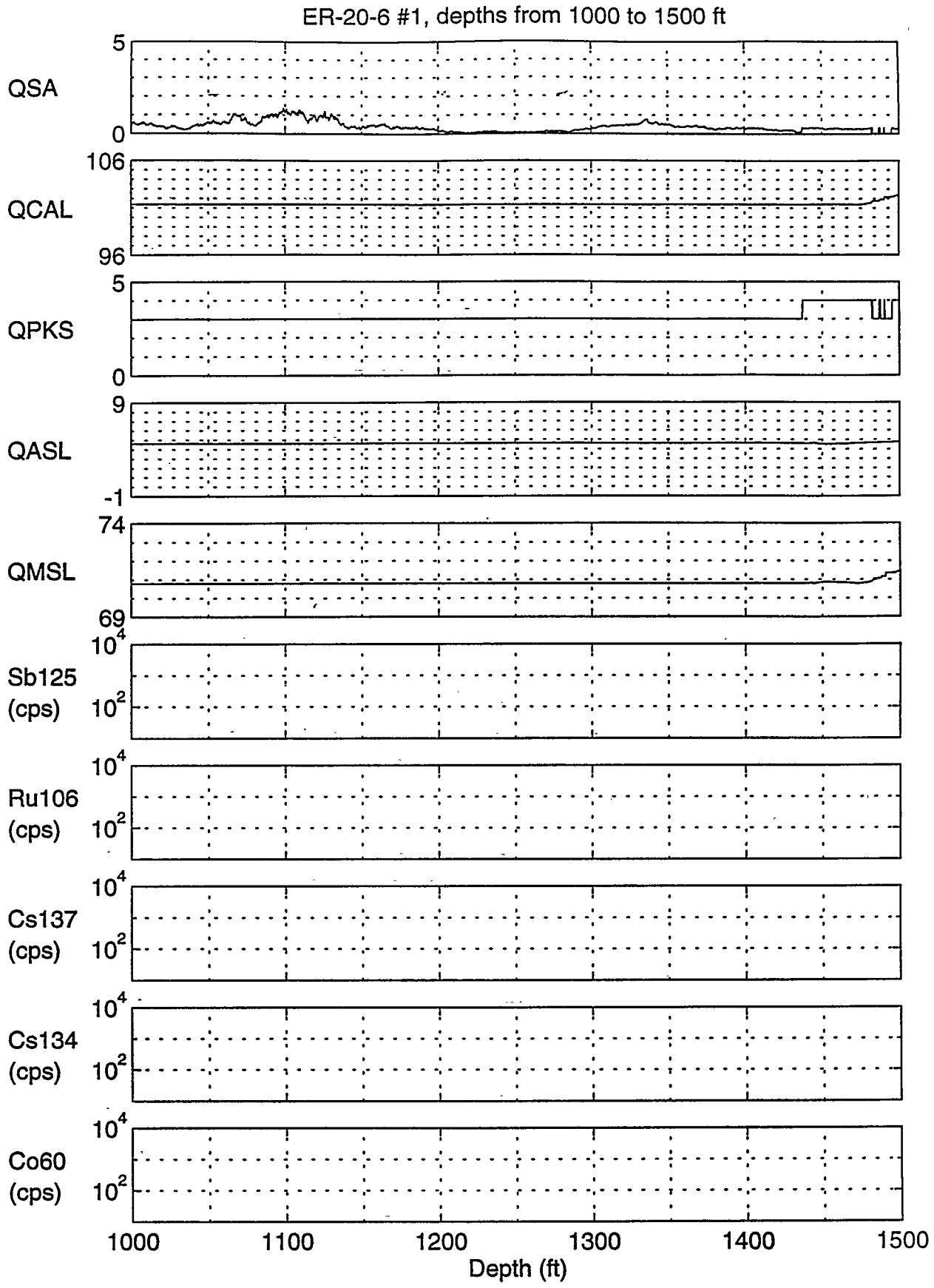

Figure 21. Western Atlas artificial nuclide data and quality control indicators for 1000-1500 ft.

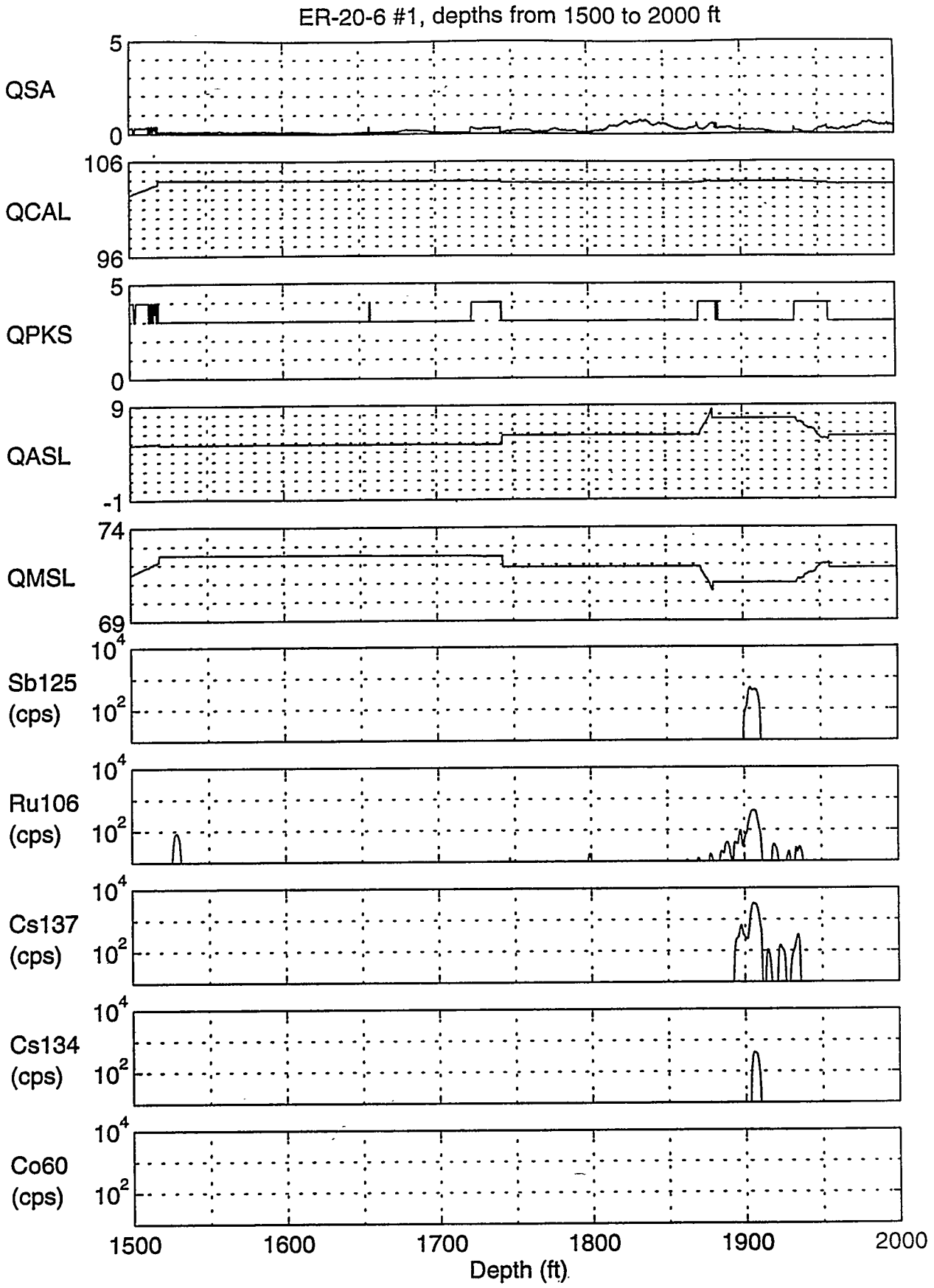

Figure 22. Western Atlas artificial nuclide data and quality control indicators for 1500-2000 ft.

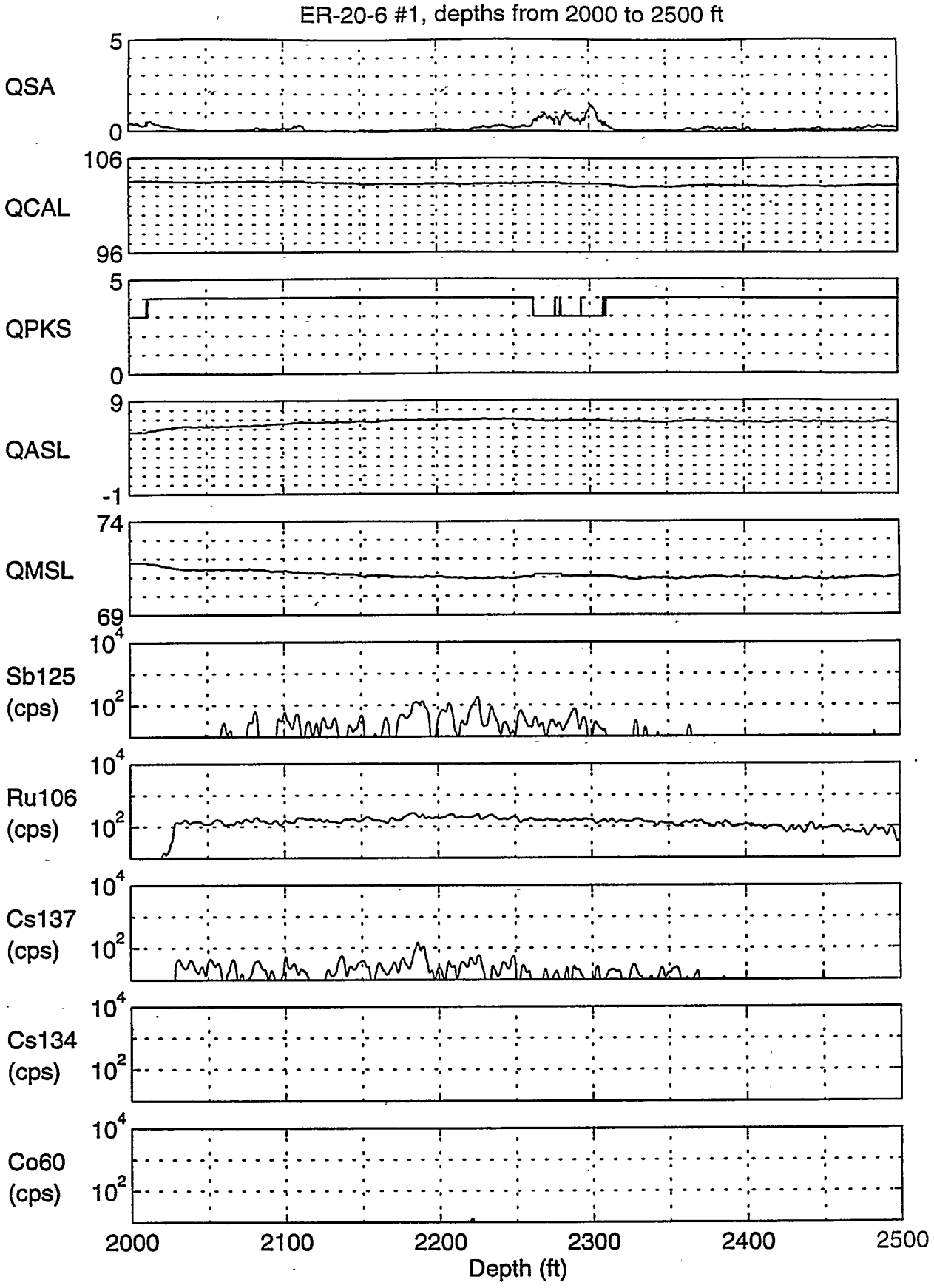

Figure 23. Western Atlas artificial nuclide data and quality control indicators for 2000-2500 ft.

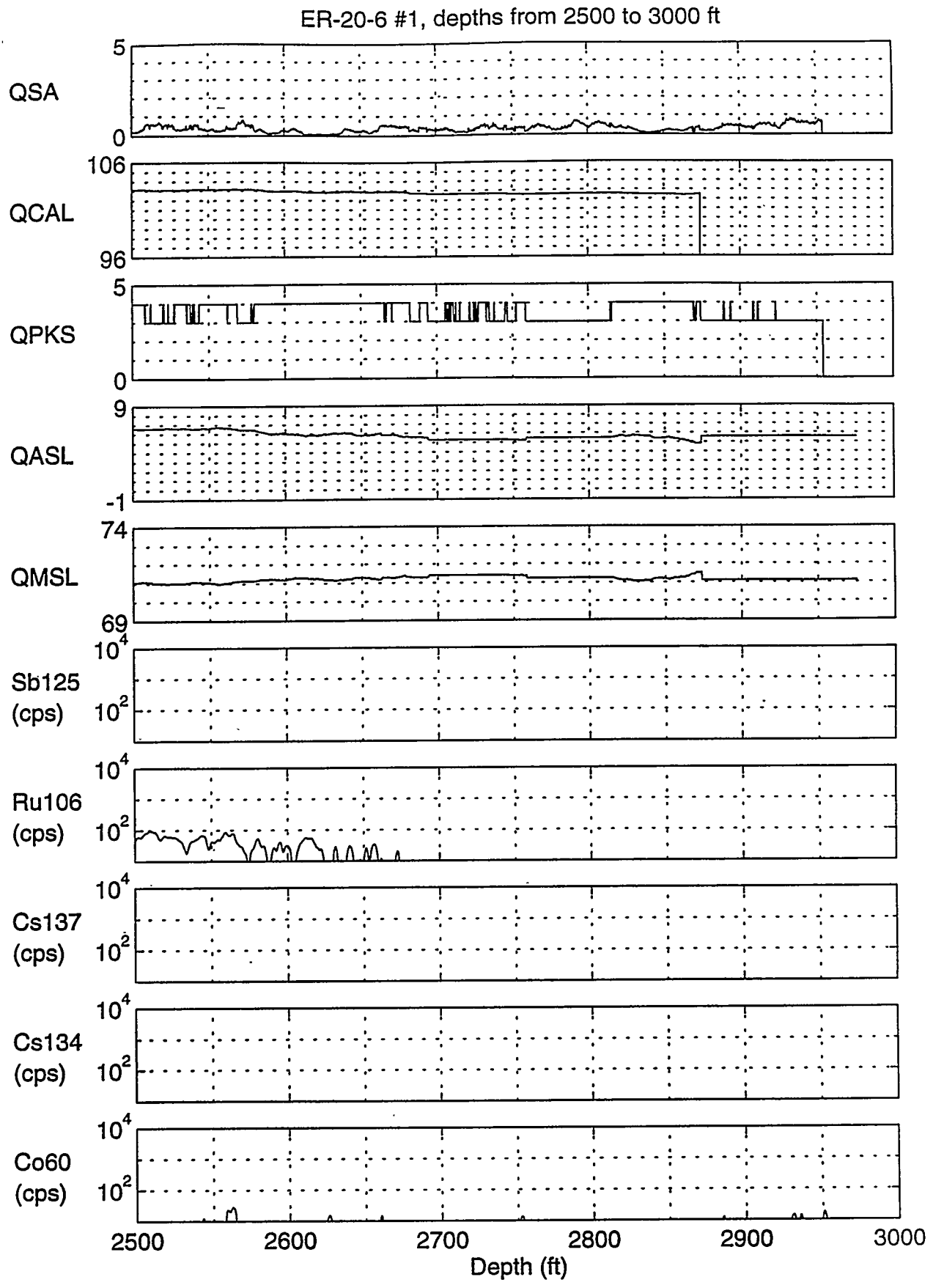

Figure 24. Western Atlas artificial nuclide data and quality control indicators for 2500-3000 ft.

Our primary recommendation for improving the results is to fix the software problem that allows photopeaks from artificial nuclides to perturb the automatic spectral recalibration in the post-processing stage.. This software fix should be relatively easily accomplished and is especially important if more boreholes are to be logged in the UGTA work. Existing borehole data should be reprocessed with the revised software.

Other changes that were recommended in an earlier report are to use the old large-detector spectral gamma-ray tool, do a better job of characterizing the logging system for NTS conditions, and run repeat runs over the entire borehole. Using the old tool would yield the greatest improvement in data quality, but would require significant effort.

REFERENCES

{1} J. Thompson in CST-7 Group Annual Report, Los Alamos National Laboratory, 1996.

{2} J.G. CONAWAY, "Identification of artificial gamma-emitting nuclides using a scintillation-based gamma-ray spectral logging system," *Fourth Annual Symposium on Borehole Geophysics for Geotechnical and Groundwater Applications*, Minerals and Geotechnical Logging Society, Toronto, August 26-30, 1991.

{3} R. Pemper, personal communication, 1996.

APPENDIX A

DATA PROCESSING SOFTWARE USED IN PREPARING THIS REPORT

The data validation was carried out largely with programs written in the MATLAB™ (for MATrix LABoratory) computer language; such programs written for the PC environment typically have a ".M" file extension and are called m-files. MATLAB is a high level programming language featuring fast development of programs with simple, powerful matrix-level commands allowing long variable names. At the time that this work was begun, MATLAB had an interpreter but not a compiler; now, a compiler is available and MATLAB programs and functions can be cross-compiled into the C language. MATLAB is very efficient for operations on an entire array at once. MATLAB has many mathematical functions built-in, with other specialized functions in modules available separately.

Data formats

The data are supplied by the contractor in the form of *bluelines*, *curve* data files, and *spectral* data files. Bluelines (as they are called in the petroleum industry) are z-fold paper plots of various log-derived parameters as a function of depth, along with log header information.

Curve data files are essentially digital (ASCII) forms of the data plotted in the various bluelines, as a function of depth, along with log header information. The data files consist of a long header followed by the logging data, which includes sample depth and twenty columns of calculated parameters including data plotted on the bluelines, energy gain and offset parameters, and various quality control indicators.

Spectral (ASCII) data files consist of a short header followed by the logging data, which includes sample depth, sample time, and a 256-channel spectrum (in counts per channel, not count rate) for each sample location in the borehole (0.25 ft intervals). The spectral data files are used by the logging contractor to produce the curve data and bluelines. To evaluate the validity of the contractor's processed results, it is essential to have access to the spectral data.

Standard programs

The overall flow of data in our standard data validation procedure is described here.

1. A visual analysis of the bluelines supplied by the contractor is performed. First, an overall quality control check is made. Calibration information is checked, and the log curves are scanned visually, looking for abnormalities or odd features that should be investigated.
2. Each recorded spectrum (in the *spectral* data file) is adjusted to the energy gain and offset values calculated by the contractor (recorded in the *curve* data file) at each sample point using the program CALSPEC.M. This is necessary because the energy scale of the spectrum can expand and contract during the logging process like a spring fixed at one end. Before summing spectra over a depth range (a later step in the processing) the spectra must all be adjusted to the same energy gain and offset. CALSPEC.M reads a complete Western Atlas spectral data file and the corresponding curve data file simultaneously, rechannelizes each spectrum based on gain (M) and offset (A) values from the curve file, and writes the adjusted

spectra in the same format as the input spectral data file (M is a multiplicative constant and A is an additive constant).

3. Next, using the blueline, the borehole is divided by the log analyst into depth ranges corresponding to radioelement characteristics reported by the logging contractor. These zones are selected as either being clean (i.e., barren of artificial gamma-emitters) or as being a zone having fairly uniform artificial nuclide composition (for example, mostly ^{106}Rb with some ^{125}Sb).
4. The spectra are summed over each of the depth ranges described above using the program STEP1.M (the program names are historical; obviously, this is no longer the first step). The program writes a separate output file for each summed spectrum. The output file names give the depth range; for example 05251250.DAT would contain a spectrum summed over the depth range from 525 feet to 1250 feet; output file names are generated automatically.
5. In an optional processing step, spectra from two or more of the depth rages summed using STEP1.M can be combined into a single spectrum. Normally, this is done to combine spectra from all clean zones in the borehole into a single file named CLEAN.DAT, or it could be done to combine spectra from other zones with similar characteristics. This step is accomplished using the program STEP2_OP.M (for step 2 optional).
6. At this stage, the spectra have been energy-calibrated, summed over specified depth ranges, and converted to counts per second. In the next step, the contributions of naturally-occurring gamma emitters are subtracted from one of these summed spectra to determine if artificial nuclides are present. This step is accomplished interactively using the program STEP3.M; the progressive subtraction begins with the thorium family, followed by the uranium family, and finally ^{40}K. We start with the thorium family because the 2.614 MeV peak from ^{208}Tl is the highest-energy peak of any nuclide that is likely to be found in quantity at the NTS. Uranium is subtracted second because, after thorium, the uranium family has the highest energy peaks. Any residual spectrum remaining after the estimated spectral contributions of the three natural radioelement families are subtracted should be attributable to artificial nuclides plus noise resulting from counting statistics and errors that creep into the results as successive processing steps are performed. The residual spectrum is plotted with each of the five artificial gamma-emitters for which Western Atlas spectral templates are available, and a visual analysis is made of the various fits.
7. If no artificial nuclides are evident in the residual spectrum produced by STEP3.M, the routine processing is finished. If substantial amounts of artificial nuclides are evident then an optional processing step can be undertaken using STEP4.M. This program allows interactive fitting of a weighted spectral template composed of the five artificial gamma-emitting nuclides for which Western Atlas has characterized their system.

APPENDIX B

POSSIBLE DEFICIENCIES IN LOGGING SYSTEM AND CONTRACTOR DATA PROCESSING

As stated in the main body of this report, the contractor does not calculate an apparent concentration for artificial nuclides so concentration errors are not an issue; deflections of the artificial nuclide curves are expressed in counts per second. That leaves three types of possible error in the artificial nuclide curves (other than a conventional measurement depth error that is always a small possibility in a logging operation): (a) artificial nuclides are indicated in the log but are not actually present, (b) artificial nuclides are present but not indicated in the log, and (c) artificial nuclides are present but misidentified as other artificial nuclides. Of these three errors, Atlas research personnel report that Type 1 errors have been observed in clean wells. Such false anomalies are a natural consequence of trying to extract small signals from noisy data. Given that type-1 errors are known to occur, it would seem unavoidable that types 2 and 3 occur as well. It is likely that the incidence of all three types of errors could be reduced by tightening the quality standards of the data processing. However, the overriding factor limiting data quality is the poor spectral resolution of the CsI detector; changing this would require a major effort.

In earlier stages of our data validation efforts, we observed a number of apparent deficiencies in the Atlas spectral gamma-ray logging equipment and data processing. This led to joint experiments at the Atlas research facility in Houston to see what effect these deficiencies might have on the results. We used the Atlas sandstone borehole model which is designed to accommodate button sources as well as the logging tool. Small calibration sources (the same five artificial nuclides for which the system was characterized) were inserted singly and in various combinations of two to provide a variety of signals. The sources were inserted in two source holes (1 in and 3 in from the borehole) while spectra were recorded on time drive, simulating logging conditions at the NTS.

We found that for experimental conditions that were essentially the same as the calibration conditions, the data processing worked well. As conditions departed from this ideal, errors increased. In general, the processing was able to identify the artificial nuclides that were actually present in any given experiment, but frequently also identified nuclides, sometimes indicating substantial quantities, that were not present. The system is able to recognize the presence of artificial nuclides fairly reliably, but sometimes misidentifies the specific constituents.

As an example, we ran one experiment where the tool was centered in the water-filled calibration block with button sources inserted one at a time into the source hole located 1 in from the borehole. This experiment differed from the calibration configuration only in that the tool was centered instead of sidewalled on the side of the borehole where the button source is located. With this small modification, a ^{137}Cs source that contributes 100 cps (counts per second) to the ^{137}Cs channel would contribute a total of 97 cps to the other seven radioelement channels. This was the worst result in this particular experiment. The best result was obtained with ^{60}Co. A ^{60}Co source that contributes 100 cps to the ^{60}Co channel would contribute a total of 55 cps to the other seven radioelement channels under these conditions.

This experiment was not the worst case by any means; a similar experiment using the source hole 3 in from the borehole for the button sources gave considerably worse results. While the tool is not normally run centered as in these two experiments, the distribution of artificial nuclides is likely to be irregular around the borehole or even in the borehole itself, which may be filled with water or air. Many different source-absorber-detector geometries are possible, some of which will produce worse results than those described above. Atlas personnel feel that the data processing is valid but the signal-to-noise problem is too extreme given the poor spectral quality{B1}; we concur. We tried manually tweaking gains and other parameters for optimal quality, but the results were as likely to deteriorate as to improve.

In summary, we found that the spectral gamma-ray logging system seems to be fairly useful for identifying the presence of artificial nuclides but can be expected to identify nuclides that are not actually present in addition to those that are. Such errors are probably an unavoidable consequence of trying to extract small signals from noisy data but steps can be taken to reduce the errors. The contractor seems to be following generally accepted professional practice although some improvements are possible. The deficiencies are discussed below.

Energy calibration. Spectral data are initially expressed in counts per second per channel for the 256-channel recorded field spectra. One of the first steps in processing the data is to perform an energy calibration, determining the appropriate multiplicative and additive calibration constants (gain and offset) so the data can be expressed as a function of gamma-ray energy rather than channel number. The energy calibration of the system tends to drift as a result of temperature changes and other factors, so the calibration factors must be updated frequently. While the energy calibrations of the spectral templates are not bad, there is room for improvement. Errors in peak position of a channel or two are common in the templates and the field data. It seems likely that improving the energy calibration would improve confidence in the nuclide identifications. In the main body of this report, we described a separate problem with the Atlas automatic peak tracking where photopeaks from artificial nuclides interfere with the natural reference peaks used for post-processing calibration on the fly. Thus, the spectral calibration can be at its worst in zones of greatest interest in the UGTA work, zones that are contaminated by artificial gamma emitters.

Background subtraction. The artificial nuclide spectral templates were obtained experimentally in a sandstone block with a 12 in diameter hole drilled through it. Additional small holes drilled from the outside of the block allow insertion of button sources. Because the sandstone itself contains natural gamma emitters, the natural background was subtracted from the experimental data to produce the spectral templates. In a few cases, this distorted the templates appreciably (Appendix C).

Incorrect borehole environment. The borehole environment affects the overall spectral shape because of differences in gamma-ray attenuation caused by the type of borehole fluid, for example, or the type of casing present, if any{B2-B4}. This category also includes differences in spectral shape resulting from the use of button sources for the artificial nuclides rather than distributed sources. A point source, a plane source and a three-dimensionally distributed source would all exhibit different spectral shapes. In a liquid-filled borehole, whether the logging instrument is centralized or sidewalled makes a significant difference in spectral shape as well.

Missing templates. It seems that not all possible gamma-emitting fission fragments and perhaps other gamma-emitting nuclides are represented by the Atlas templates. For example, ^{102m}Rh was found in water samples from ER20-6 #1 (see Table 1 in the main body of this report) and other fission products such as ^{144}Ce and its short-lived daughter ^{144}Pr have several gamma-ray lines with relative intensities on the order of one per cent. While these are relatively weak lines, the nuclides could be present at activities an order of magnitude or more greater than, say, ^{106}Ru[B5]. Any artificial gamma emitters present in significant quantities but not included in the data processing would probably lead to erroneous nuclide identifications. This is a subject for a nuclear chemist to consider.

Blueline curve smoothing. The contractor applies a smoothing filter to the radioelement curve data presented in the bluelines (hard-copy plots). Following smoothing, a single-point anomaly on the processed log would have a smooth, bell shape. While an unsmoothed spike might stand out as a likely erroneous data point (no distribution of radioelements will produce a substantial one-point anomaly), a smooth, bell-shaped anomaly appears more credible to the eye because this is the way a real anomaly would appear. This is a subjective factor that data users should keep in mind. Similarly, negative concentrations are a natural artifact of the data processing procedures in the presence of noise, but the contractor discards negative values and adjusts the curve so it smoothly approaches zero in those zones; from the standpoint of log quality control, I would prefer to see the negative values.

Differential non-linearity. Pronounced differential non-linearity was observed in the Western Atlas spectra (Figure B1). The detector in the standard Atlas SGR tool is 2" x 12" CsI with a 12-bit successive approximation analog-to-digital-converter (ADC). Only the 8 most significant bits are used, and the data are transmitted up the logging cable in digital form. Generally, the specification on successive approximation converters is ±1/2 of the least significant bit. When such an ADC is used for spectrometry, this can lead to errors in channel width of ±100%, that is, a given channel can vary from zero width (never receives any counts) to double the nominal width. By using the 8 most significant bits of a 12-bit ADC, the maximum error in channel width is reduced from ±100% to ±6.25%. This is a big improvement but, in our experience, is still not an acceptable noise level for addressing the difficult problems at the NTS.

REFERENCES FOR APPENDIX B

{B1} D. Oliver and R. Pemper, personal communication, 1996.

{B2} J.G. CONAWAY, K.V. ALLEN, Y.B. BLANCHARD, Q. BRISTOW, W.B. HYATT, AND P.G. KILLEEN, "The effects of borehole diameter, borehole fluid and casing thickness on gamma ray logs in large diameter boreholes." In *Geol. Surv. Can. Paper 79-1C*, p. 37-40 (1979).

{B3} R.D. WILSON, D. C. STROMSWOLD, M. L. EVANS, M. JAIN and D. A. CLOSE, "Spectral gamma-ray logging II: Borehole correction factors," In *Trans. Society of Professional Well Log Analysts Annual Logging Symposium*, Tulsa, paper EE (1979).

{B4} J.A. CZUBEK, "Influence of borehole construction on the results of spectral gamma-logging," In *Nuclear Techniques and Mineral Resources*, IAEA Proceedings Series, IAEA, Vienna (1969).

{B5} C.F. Hunter and N.E. Ballou, "Fission-product decay rates. *Nucleonics* V. 5, p. C2-C7, 1951.

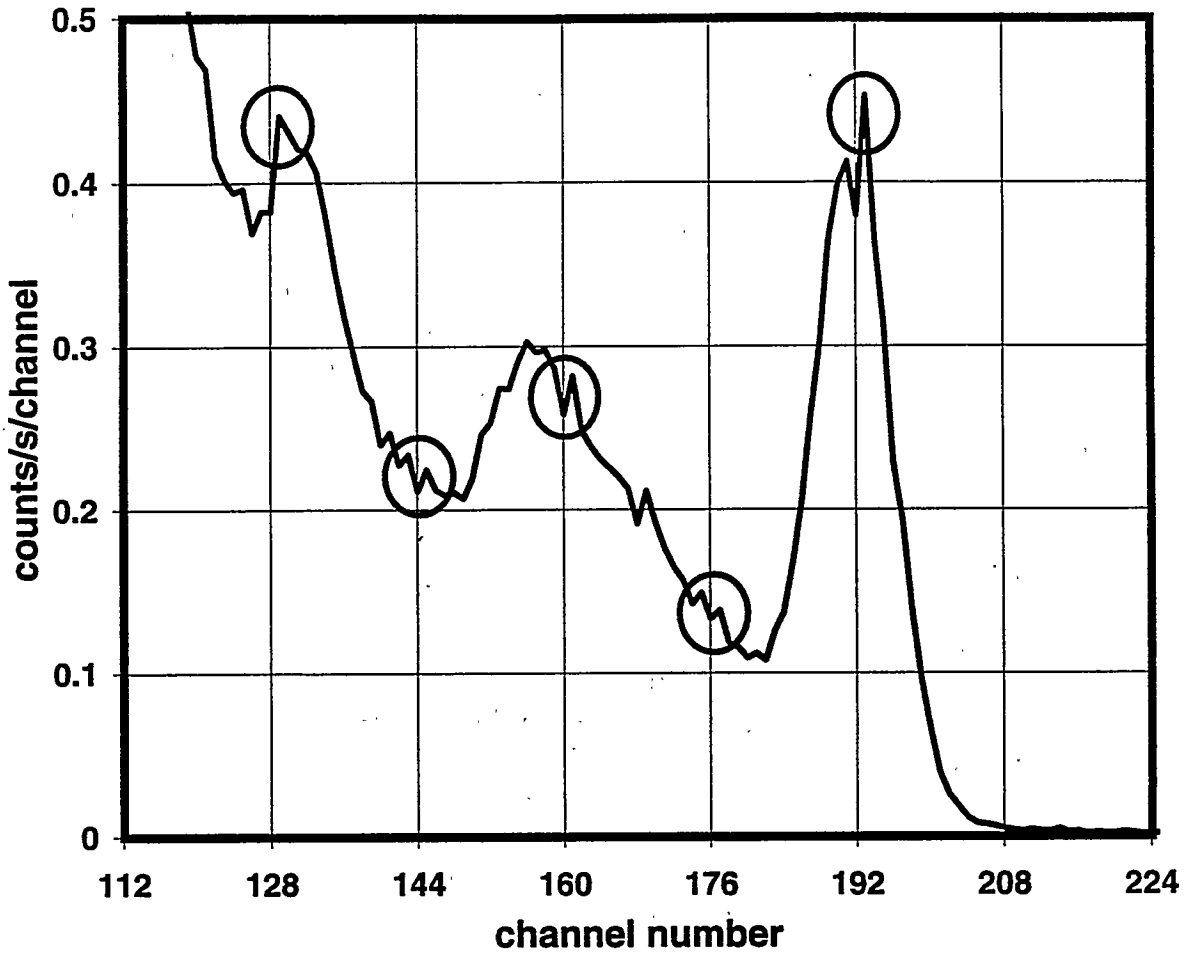

Figure B-1. We diagnosed differential non-linearity in the Western Atlas spectral gamma-ray tool based on examination of accumulated spectra such as the portion shown here. The characteristic positive-negative spike pairs show up at regular channel intervals, in this case 16 channels. This problem could be minimized with better hardware design but is not amenable to correction by post-processing.

APPENDIX C
SPECTRAL TEMPLATES

The energy calibrations of the spectral templates seem to vary by a channel or two. A good approach to determining the energy gain and offset calibration parameters is to determine the centroid of several photopeaks (after background subtraction) and use a least squares fit of centroid channel versus energy to determine the appropriate gain and offset values. The fact that peak shape varies with energy and is not truly Gaussian must be kept in mind during this procedure and adjustments made if required.

The spectral templates supplied by Atlas are shown in Figures C1 - C6. In some of these figures representing more complex spectra, two curves are shown. In these cases the lower curve is the spectral template and the upper curve is a simulated spectrum produced by a program called SYNTH™, developed at Pacific Northwest National Laboratory. The simulated spectra are not intended to reproduce the experimental data but rather are used to allow a quick visual check of the energy calibrations. Another visual check of the energy calibrations is provided by vertical dashed lines located at prominent photopeak energies.

In some of the spectral templates it is not feasible to evaluate the accuracy of the energy gain and offset parameters independently because there may be only one photopeak or, in the case of multiple photopeaks, they may be too closely grouped to get an accurate assessment. In these cases we can only determine if the gain and offset, taken together, produce accurate peak positions. This may not be adequate because the Comptom continuum located at lower energies may be shifted, potentially causing processing errors for lower energy peaks of interest.

Potassium, uranium and thorium. Figure C1 shows the following templates: (a) potassium (^{40}K), (b) uranium and daughters, and (c) thorium and daughters, plotted using the contractor's default gain and offset values. The uranium and thorium plots show two curves each, the lower curve being the contractor's template while the upper curve is the simulated spectrum produced as a check on the contractor's energy calibration, as explained above. The potassium, uranium, and thorium templates are spectra obtained in model boreholes established by the American Petroleum Institute (API) for use by oil companies and service contractors[C1]. These boreholes have a diameter of 8.5 in while the boreholes being logged at the NTS have a nominal diameter of 12.25 in. Atlas personnel use these three templates with their least-squares processing routine to estimate the contribution of K, U, and Th to the field spectra. Visual inspection of the potassium template (a) shows that the default gain/offset combination produces a peak position that may be slightly offset to the left (lower energy). Inspection of the uranium template (b) indicates the gain and offset are essentially correct. The peaks in the thorium template (c) appear to be offset slightly to the left (lower energy).

^{125}Sb. Figure C2 shows three different spectral templates for ^{125}Sb. All of the artificial nuclide templates were produced using a small 'button' source. For each artificial nuclide, three spectra were obtained.

1. The logging instrument in a sandstone block with a 12 in diameter air-filled hole drilled through it, the button source located 3 in inside the borehole wall in a small hole drilled from

the outside of the block (plot a). The contractor uses this template in each case to represent the respective artificial nuclide spectra, based on the observation that it seems to represent the best fit to the field data.

2. The logging instrument in the same sandstone block but with the button source located 1 in inside the borehole wall in a small hole drilled from the outside of the block (plot b).
3. The logging instrument hanging in air with the button source about 13 in from the pressure housing (plot c).

A background spectrum was collected and subtracted from the artificial nuclide templates with the goal that each template represent only the contribution of one of the nuclide families listed above. Each of these three templates appears to be offset slightly to the left (lower energy).

^{106}Ru. Figure C3 shows three different spectral templates for ^{106}Ru, as described above for ^{125}Sb. Templates (a) and (c) show the effects of an inaccurate background subtracted – these two templates have been overcorrected for background. The energy calibration of the template that the contractor uses for routine processing (plot b lower curve) appears to agree fairly well with the simulated spectrum (upper curve).

^{137}Cs. Figure C4 shows three different spectral templates for ^{137}Cs, as described earlier for ^{125}Sb. ^{137}Cs is a monoenergetic source. The position of the 0.662 MeV photopeak for the template that the contractor uses for routine processing (plot b) appears to be shifted slightly to the left (lower energy).

^{134}Cs. Figure C5 shows three different spectral templates for ^{134}Cs, as described earlier for ^{125}Sb. The energy calibration of the template that the contractor uses for routine processing (plot b lower curve) appears to agree fairly well with the simulated spectrum (upper curve), although the nominal gain may be slightly low based on observation of the three most prominent peaks.

^{60}Co. Figure C6 shows three different spectral templates for ^{60}Co, as described earlier for ^{125}Sb. ^{60}Co emits gamma rays at two characteristic energies, 1.17 and 1.33 MeV. The energy calibration of the template that the contractor uses for routine processing (plot b) appears to be approximately correct.

This analysis of the gain and offset of the contractor's spectral templates is far from rigorous. While one could argue over the details of this analysis, however, there does appear to be some inconsistency in the energy calibration of these templates. In the case of the monoenergetic sources (^{40}K and ^{137}Cs) and the sources with no prominent low-energy peaks (especially ^{60}Co) the gain and offset can be evaluated as a combination but not separately. The danger here is that if the gain and offset are not correct, the low-energy continuum will not have the correct shape for least-squares fitting to the field spectra.

The importance of accurate energy calibration for the spectral templates and field spectra is demonstrated in Figure C7, where five spectral templates for the five artificial gamma emitters are plotted together. The low-energy continuum around 0.2 MeV is very similar for all five nuclides so the post-processing algorithm must rely on precise peak shapes and positions if nuclide identifications are to be accurate. This is a difficult problem when dealing with this array of relatively broad, overlapping peaks.

REFERENCES FOR APPENDIX C

{C1} H. D. Scott, Analysis of samples from the API K-U-Th logging calibration facility. Transactions Soc. Prof. Well Log Analysts 30th Annual Logging Symposium, paper MM, 1996.

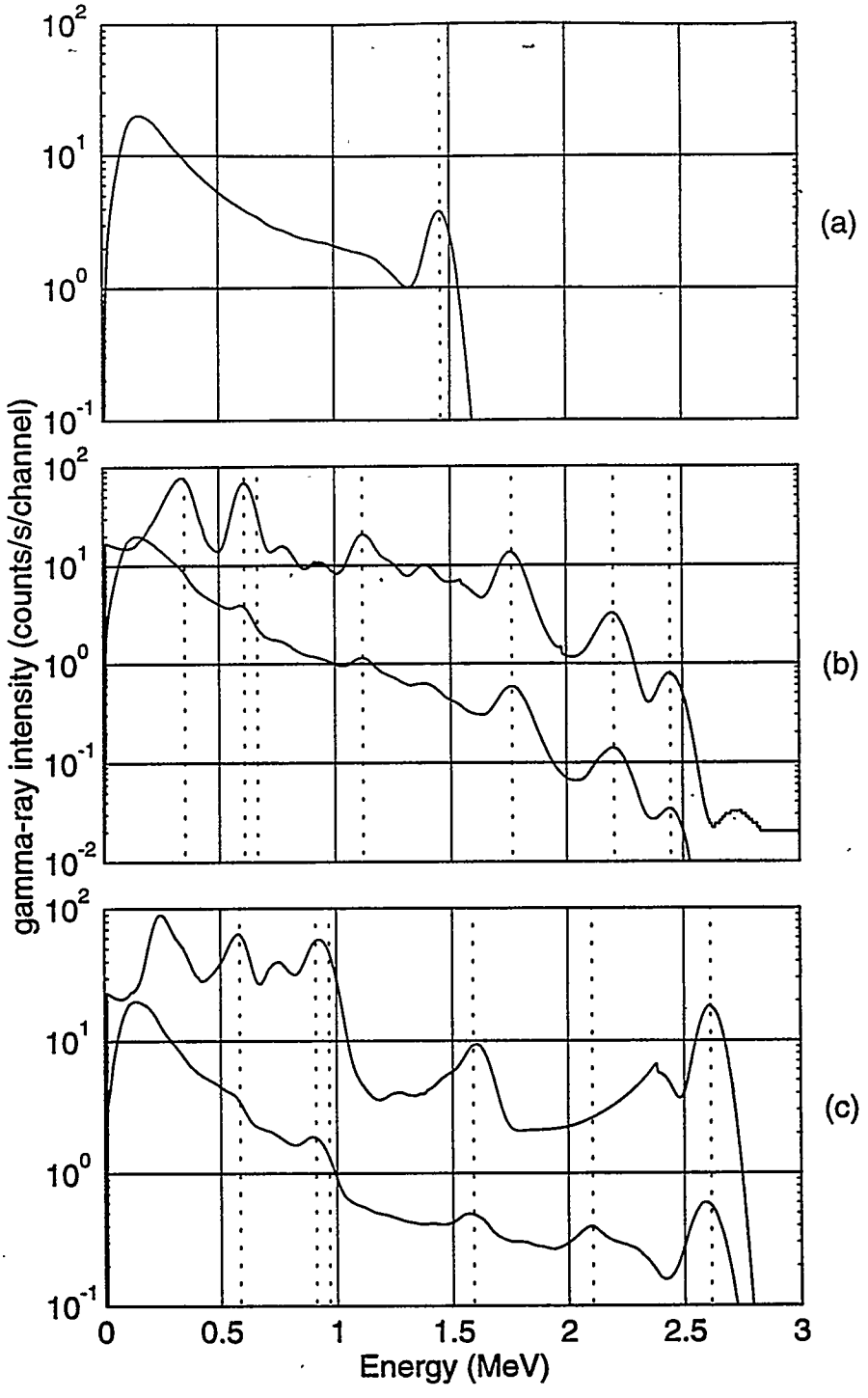

Figure C-1. Western Atlas spectral templates for (a) potassium (b) uranium, and (c) thorium. The upper curve in (b) and (c) is the corresponding simulated spectrum produced as a check on the contractor's energy calibration, as explained in the text.

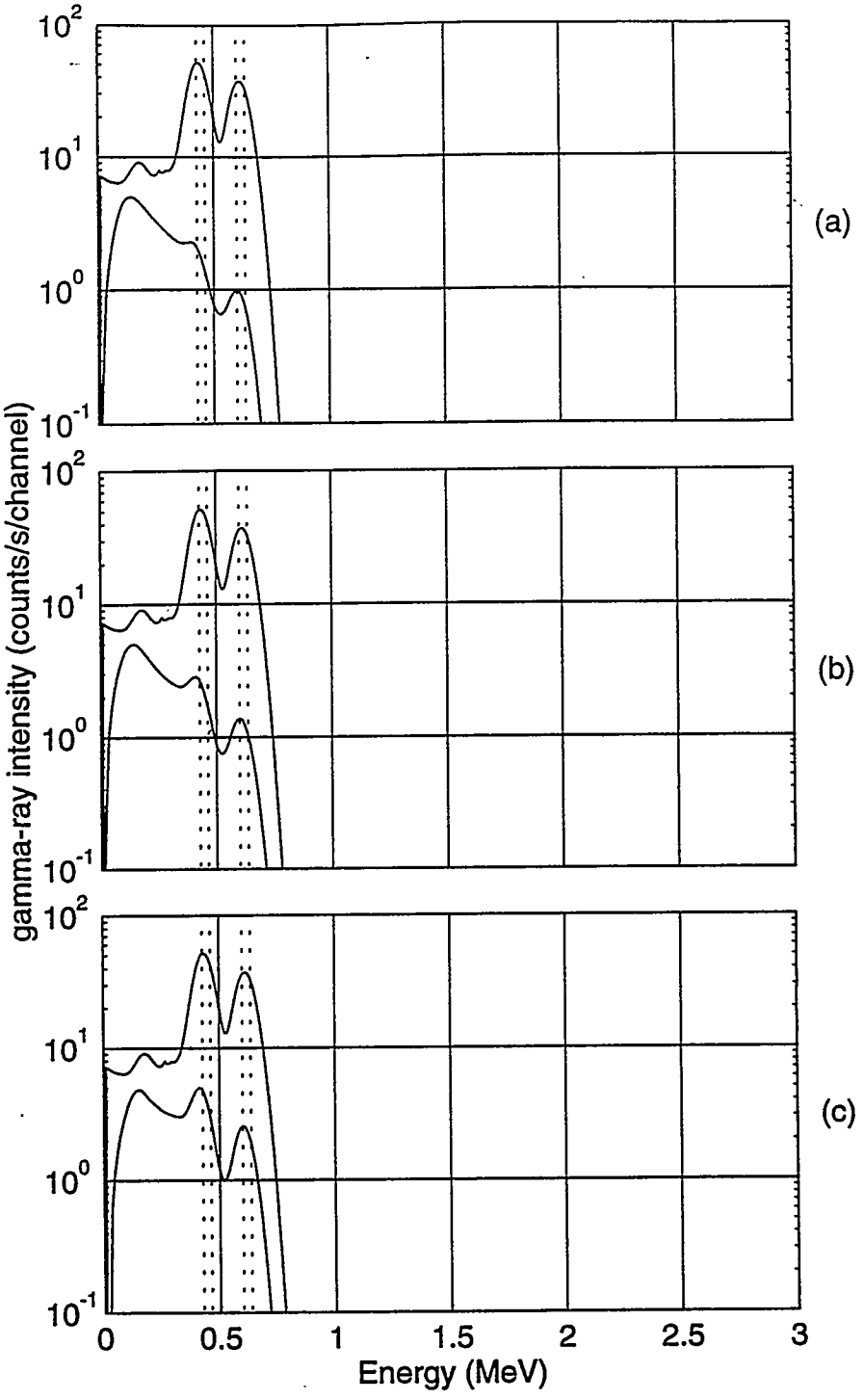

Figure C-2. Western Atlas spectral templates for ^{125}Sb with (a) button source located 1 in inside the borehole wall in a small hole drilled from the outside of the block, (b) button source located 3 in inside the borehole wall, and (c) logging instrument hanging in air with the button source about 13 in from the pressure housing. The upper curve in each case is the corresponding simulated spectrum produced as a check on the contractor's energy calibration, as explained in the text.

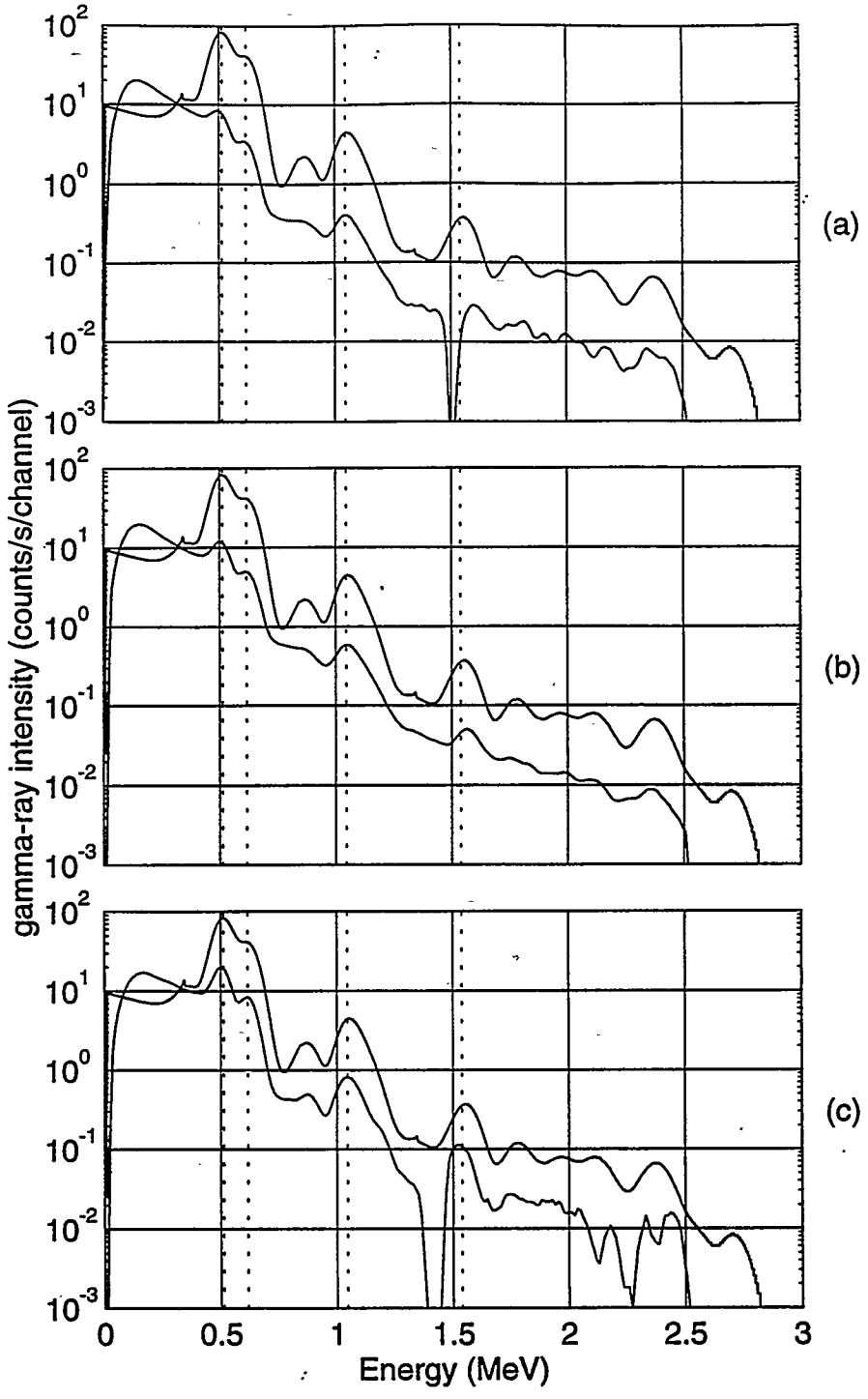

Figure C-3. Western Atlas spectral templates for ^{106}Ru with (a) button source located 1 in inside the borehole wall in a small hole drilled from the outside of the block, (b) button source located 3 in inside the borehole wall, and (c) logging instrument hanging in air with the button source about 13 in from the pressure housing. The upper curve in each case is the corresponding simulated spectrum produced as a check on the contractor's energy calibration, as explained in the text.

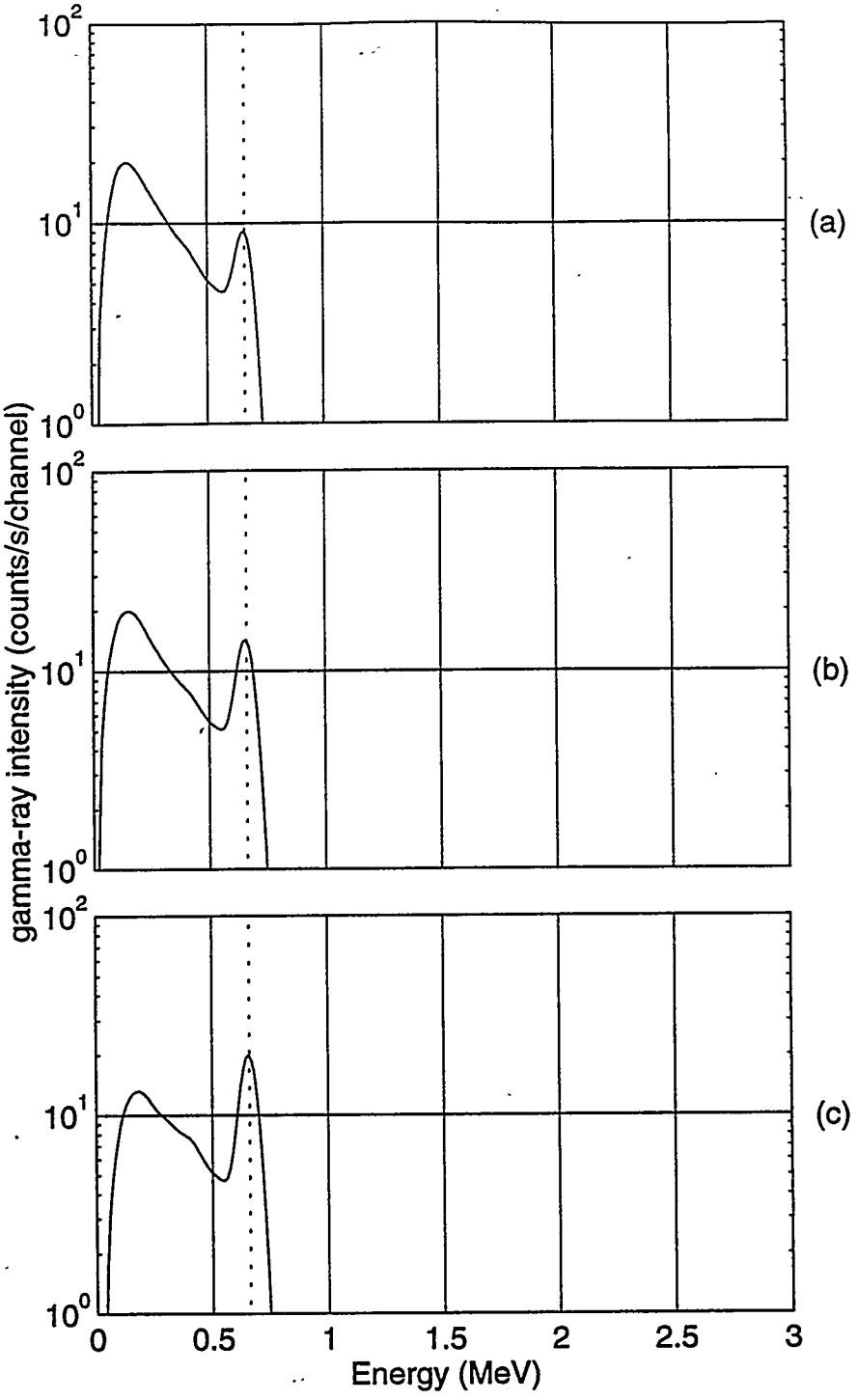

Figure C-4. Western Atlas spectral templates for ^{137}Cs with (a) button source located 1 in inside the borehole wall in a small hole drilled from the outside of the block, (b) button source located 3 in inside the borehole wall, and (c) logging instrument hanging in air with the button source about 13 in from the pressure housing.

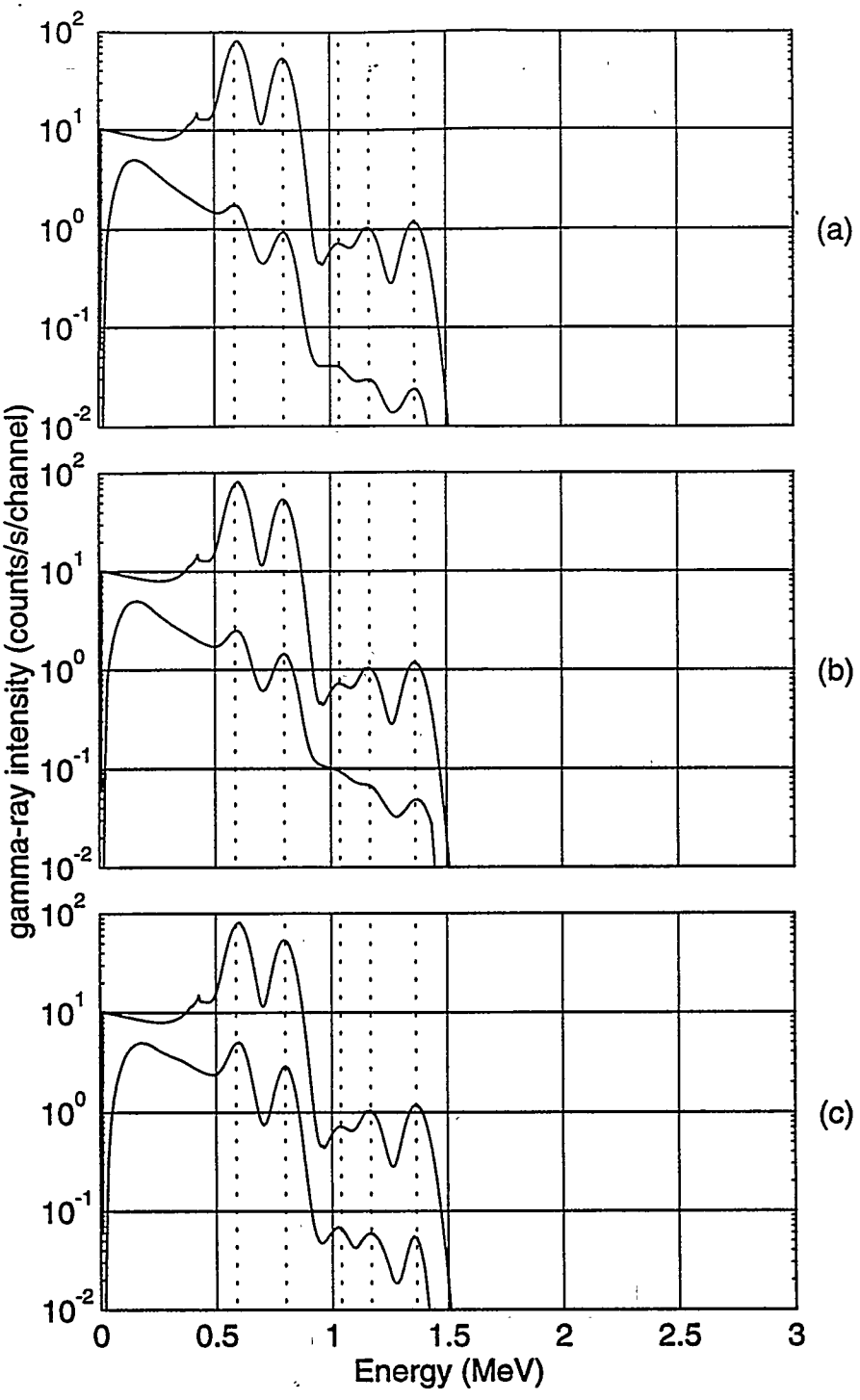

Figure C-5. Western Atlas spectral templates for ^{134}Cs with (a) button source located 1 in inside the borehole wall in a small hole drilled from the outside of the block, (b) button source located 3 in inside the borehole wall, and (c) logging instrument hanging in air with the button source about 13 in from the pressure housing. The upper curve in each case is the corresponding simulated spectrum produced as a check on the contractor's energy calibration, as explained in the text.

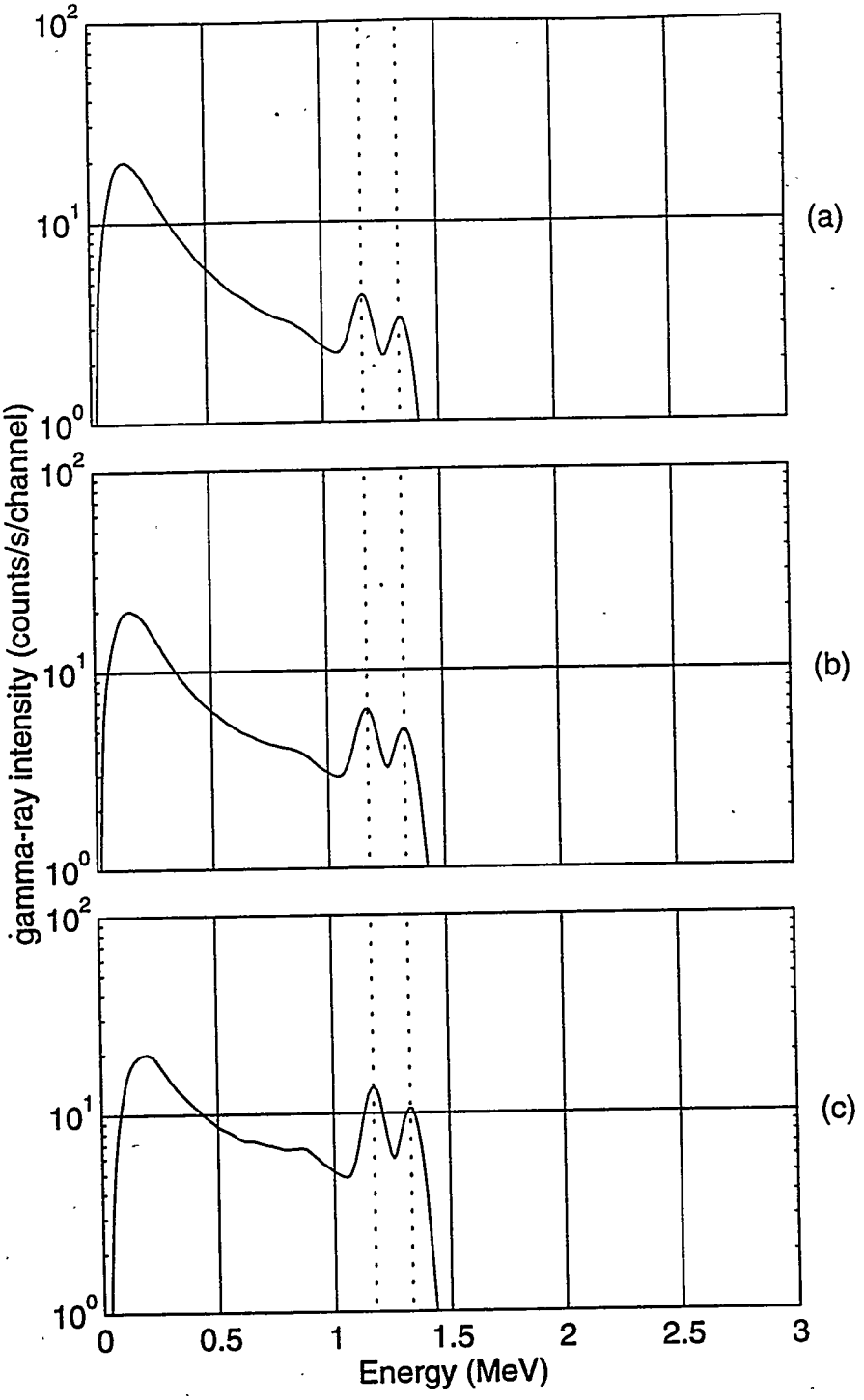

Figure C-6. Western Atlas spectral templates for ^{60}Co with (a) button source located 1 in inside the borehole wall in a small hole drilled from the outside of the block, (b) button source located 3 in inside the borehole wall, and (c) logging instrument hanging in air with the button source about 13 in from the pressure housing.

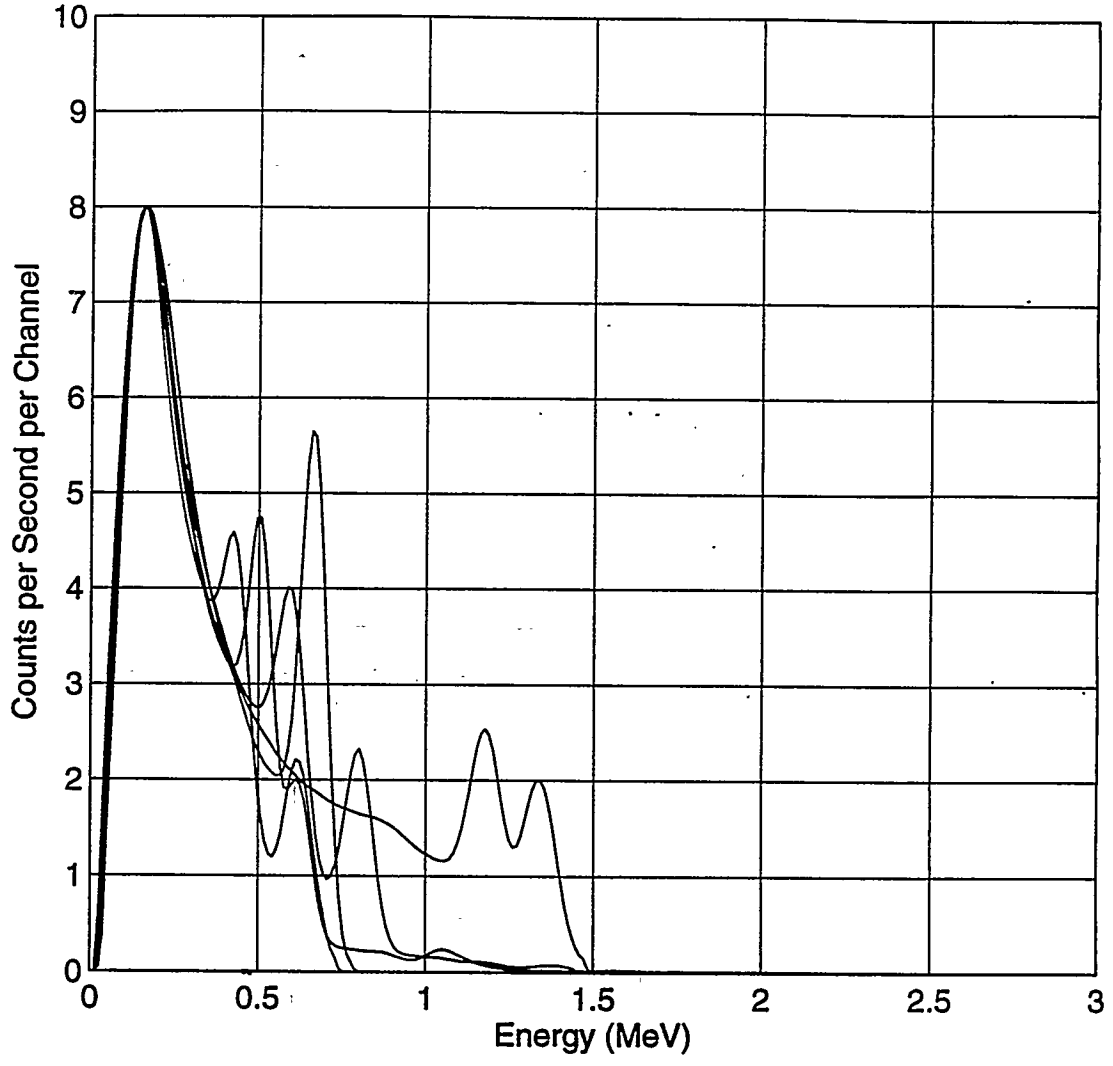

Figure C-7. Spectral templates for all five artificial nuclides plotted together. In each case, the button source was located in the source hole 1 in from the borehole.